



Investigation of 3-sulfamoyl coumarins against cancer-related IX and XII isoforms of human carbonic anhydrase as well as cancer cells leads to the discovery of 2-oxo-2*H*-benzo[*h*]chromene-3-sulfonamide – A new caspase-activating proapoptotic agent



Dmitry Dar'in ^a, Grigory Kantin ^a, Stanislav Kalinin ^a, Tatiana Sharonova ^a, Alexander Bunev ^b, Gennady I. Ostapenko ^b, Alessio Nocentini ^c, Vladimir Sharoyko ^a, Claudiu T. Supuran ^{c, **}, Mikhail Krasavin ^{a, *}

^a Saint Petersburg State University, Saint Petersburg, 199034, Russian Federation

^b Medicinal Chemistry Center, Togliatti State University, Togliatti, 445020, Russian Federation

^c Neurofarba Department, Universita Degli Studi di Firenze, Florence, 50019, Italy

ARTICLE INFO

Article history:

Received 30 April 2021

Received in revised form

23 May 2021

Accepted 27 May 2021

Available online 10 June 2021

Keywords:

Carbonic anhydrase
Enzyme inhibitors
Antiproliferative agents
Primary sulfonamides
Coumarins
Stopped-flow assay
Nanomolar inhibition
Cancer cells
MTT-Test
Hypoxic environment
Apoptosis induction
Caspase activation

ABSTRACT

Herein we report the synthesis of a set of seventeen 3-sulfonamide substituted coumarin derivatives. Prepared compounds were tested *in vitro* for inhibition of four physiologically relevant isoforms of the metalloenzyme human carbonic anhydrase (*hCA*, EC 4.2.1.1). Several coumarin sulfonamides displayed low nanomolar K_i values against therapeutically relevant *hCA* II, IX, and XII, whereas they did not potently inhibit *hCA* I. Some of these compounds exerted a concentration-dependent antiproliferative action toward RT4 human bladder cancer and especially A431 human epidermoid carcinoma cell lines. In the meantime, the viability of non-tumorigenic hTERT immortalized human foreskin fibroblast cell line Bj-5ta was not significantly affected by the obtained derivatives. Interestingly, compound **10q** (2-oxo-2*H*-benzo[*h*]chromene-3-sulfonamide) showed a profound and selective dose-dependent inhibition of A431 cell growth with low nanomolar IC_{50} values. We demonstrated that **10q** possessed a concentration-dependent apoptosis induction activity associated with caspase 3/7 activation in cancer cells. As carbonic anhydrase isoforms in question were not potently inhibited by this compound, its antiproliferative effects likely involve other mechanisms, such as DNA intercalation. Compound **10q** clearly represents a viable lead for further development of new-generation anticancer agents.

© 2021 Elsevier Masson SAS. All rights reserved.

1. Introduction

Carbon dioxide and bicarbonate ion are crucial species in biochemical processes and their interconversion has paramount significance in all living organisms [1]. Carbonic anhydrases (CA, EC 4.2.1.1) comprise a superfamily of metalloenzymes that catalyze the reversible hydration of carbon dioxide ($CO_2 + H_2O \rightleftharpoons HCO_3^- + H^+$)

and therefore govern the major physiological buffering system [1–3]. These enzymes have been found across all kingdoms of life and eight evolutionary unrelated gene families have been identified so far, including α -, β -, γ -, δ -, ζ -, η -, θ , and ι -CAs [4–8]. In human, CAs are represented by 15 isoforms (incorporating Zn^{2+} as catalytic ion and attributed to the α -class) which differ significantly in their catalytic activity, tissue distribution and subcellular localization [9,10]. Thus, cytosolic (I, II, III, VII, XIII), mitochondrial (VA, VB) secreted (VI), and membrane-associated (IV, IX, XII, XIV) human (*h*) CA isozymes have been described [11,12]. Therefore, these enzymes are essential for a wide spectrum of biological processes requiring acid-base balance be it in subcellular compartments or across the plasma membrane [13]. Interestingly, aberrant expression/activity

* Corresponding author.

** Corresponding author.

E-mail addresses: claudiu.supuran@unifi.it (C.T. Supuran), m.krasavin@spbu.ru (M. Krasavin).

of many *hCA*s is associated to disease states, which include glaucoma, edema, obesity, neuropathic pain, osteoporosis, etc. [14–20]. Hence, many *hCA* isoforms have been validated as valuable therapeutic targets and novel links to pathological disorders continue to be discovered [21–23]. Particularly, recent decades were marked with validation of the membrane-associated isozymes *hCA* IX and XII as anticancer therapeutic targets [24]. In fact, it has been demonstrated that these surficial proteins are largely overexpressed in hypoxic solid tumors where they play pivotal roles in microenvironment regulation, thus being instrumental in the survival, proliferation, metastasis and development of drug resistance of malignant cells [13,25–27]. In the light of these facts, intensive efforts are being made to bring such agents to clinical use for the needs of diagnostic, theranostic, and combination therapy of solid tumors [28,29]. Significant progress has been achieved in the development of diagnostic tools based on *hCA* IX/XII targeting biologics and small molecules, furnishing several drug candidates on advanced stages of clinical trials [30,31]. In the meantime, cancer therapeutic agents blocking the activity of these enzymes are somewhat lagging behind with only SLC-0111 *hCA* IX/XII inhibitor entering phase II of clinical studies [24]. Therefore, ongoing efforts focused on the discovery of *hCA* IX/XII-blocking small molecules are of significant importance [24]. Moreover, supremely desired is the development of isoform-selective inhibitors i.e. uncomplicated with high affinity to the ubiquitous cytosolic isozymes *hCA* I and II [32].

The vast majority of highly potent and selective *hCA* IX/XII inhibitors known so far (including those studied in preclinical and clinical settings) belong to two dominant classes of *hCA*-blocking compounds. Thus, most of isoform-selective nanomolar inhibitors, such as *hCA* IX/XII specific SLC-0111 and indane sulfonamide **1** (Fig. 1), represent the class of 'Zn-binders' which exert their *hCA* inhibitory effect via coordination to the catalytic Zn²⁺ ion situated at the bottom of the enzyme's active site. Such mechanism is characteristic to primary sulfonamide-based *hCA* inhibitors, as well as their bioisosters (sulfamides, sulfamates) [33]. It has been shown that while the Zinc binding warhead anchors in depth of the catalytic cleft (whose structure is highly conservative across all *hCA* isoforms), molecular periphery of efficient inhibitors is capable of binding at the entrance of the active site [9,34,35]. Noticeably this outer rim of the catalytic cavity is outlined with certain number of non-conservative amino acid residues and therefore isoform selectivity can be achieved on the way to safe and efficient therapeutic agents [36]. Another well explored class of *hCA* inhibitors is represented by coumarin-based "prodrugs" which were found to occlude the entrance of the catalytic cleft after being catalytically hydrolyzed within the *hCA* active site [37]. Importantly, the resulting derivatives of 2-hydroxycinnamic acid interact with the outer rim of the cavity (mainly forming van der Waals contacts with hydrophobic amino acid residues [38]) rendering this class of inhibitors sensitive to the differences in the active site architecture between different enzyme isoforms [39]. Schematic representation of the described mechanisms of *hCA* inhibition is outlined in Fig. 1 (A, B) along with *hCA* IX/XII-specific compounds SLC-0111, **1**, **2**, and **3** exemplifying the corresponding chemotypes (C) [37,40–42].

Interestingly, while analyzing the emerging publications on this issue, we have noticed that a number of efficient *hCA* inhibitors have been recently reported which were designed through linking of sulfonamide and coumarin warheads within one molecule [43–47]. Furthermore, recent review highlighted the anticancer potential of such chimeric compounds which is often claimed to be attributive of the inhibition of tumor-associated *hCA* IX and XII isoforms (Fig. 2) [48].

However, the majority of these agents turned out to have rather high molecular weights, partly due to the presence of somewhat

bulky linker fragments, which can be considered unfavorable for further medicinal chemistry optimization of such hit-compounds [49,50]. In this context, we found it attractive to perform direct merging of sulfonamide moiety to the coumarin scaffold which appeared to be feasible via introduction of 2-sulfamoylacetic acid esters into the classical Knoevenagel condensation with salicylaldehyde derivatives [51]. Thus, herein we report the preparation, *hCA* inhibitory profiling and anticancer properties evaluation of seventeen hitherto undescribed coumarin derivatives incorporating primary sulfonamide group at their 3 position. In addition, detailed characterization of anticancer potential of the synthesized compounds is provided.

2. Results and discussion

2.1. Chemistry

The proposed synthetic approach furnishing the desired 3-sulfamoylcoumarins relied on the introduction of ethyl 2-sulfamoylacetate **7** into the canonical reaction of α -CH-acidic carboxylic acid derivatives with salicylaldehydes **8** [52]. To this end, reagent **7** was synthesized from commercial ethyl 2-(chlorosulfonyl)acetate **9** according to a modified literature procedure [53] (Scheme 1).

Thus obtained reagent **7** was then mixed with variously substituted salicylaldehydes **8a–q** in *n*-butanol to give the target 3-sulfamoylcoumarins **10a–q** after stirring for 2–6 h at 110 °C under basic conditions (Scheme 2).

Following the developed protocol, seventeen variously substituted 3-sulfamoylcoumarins **10a–q** were generated which represented a novel type of potential *hCA* inhibitors. Interestingly, the products' yields exceeded 60% for the unsubstituted **10a**, as well as for the derivatives bearing electron donating substituents. In the meantime, several compounds were only obtained in modest to medium yields, which included 6-nitro- (**10j**, 41%), 6,8-dichloro (**10k**, 30%), and naphthalene (**10q**, 33%) derivatives.

2.2. Carbonic anhydrase inhibition

With regards to evaluate *hCA* inhibitory activities of the obtained compounds **10a–q** the stopped-flow carbon dioxide hydrase assay was employed, and acetazolamide (AAZ) was used as a reference drug [54]. The profiling was performed on a panel of four physiologically significant *hCA* isoforms, which comprised two ubiquitously expressed cytosolic proteins *hCA* I and II and two transmembrane tumor-associated enzymes *hCA* IX and XII. The inhibitory profile of small molecules against those isozymes is of interest with regards to different fields of medicinal chemistry [9,24,55]. Thus, *hCA* IX (and XII) proved valuable extracellular tumor biomarkers and their inhibitors attract growing attention for the needs of cancers treatment and prognosis (*vide supra*) [14,31,56]. On the other hand, *hCA* II and XII are known to govern the aqueous humor secretion in eye and therefore represent validated targets for intraocular pressure-lowering agents [19]. Otherwise, cytosolic *hCA* I is considered an off-target protein for both antiglaucoma and anticancer therapeutic applications of CAIs [57]. Inhibition constant (K_i) values of the synthesized compounds against these four proteins are presented in Table 1.

Analysis of the inhibition data outlined in Table 1 highlighted the following SAR trends:

- (i) As evident from Table 1, unsubstituted 3-sulfamoylcoumarin **10a** displayed medium inhibitory potency against *hCA* I, II and XII with K_i values of 481.6, 232.4, and 137.5 nM correspondingly. Meanwhile, higher affinity was observed for **10a**

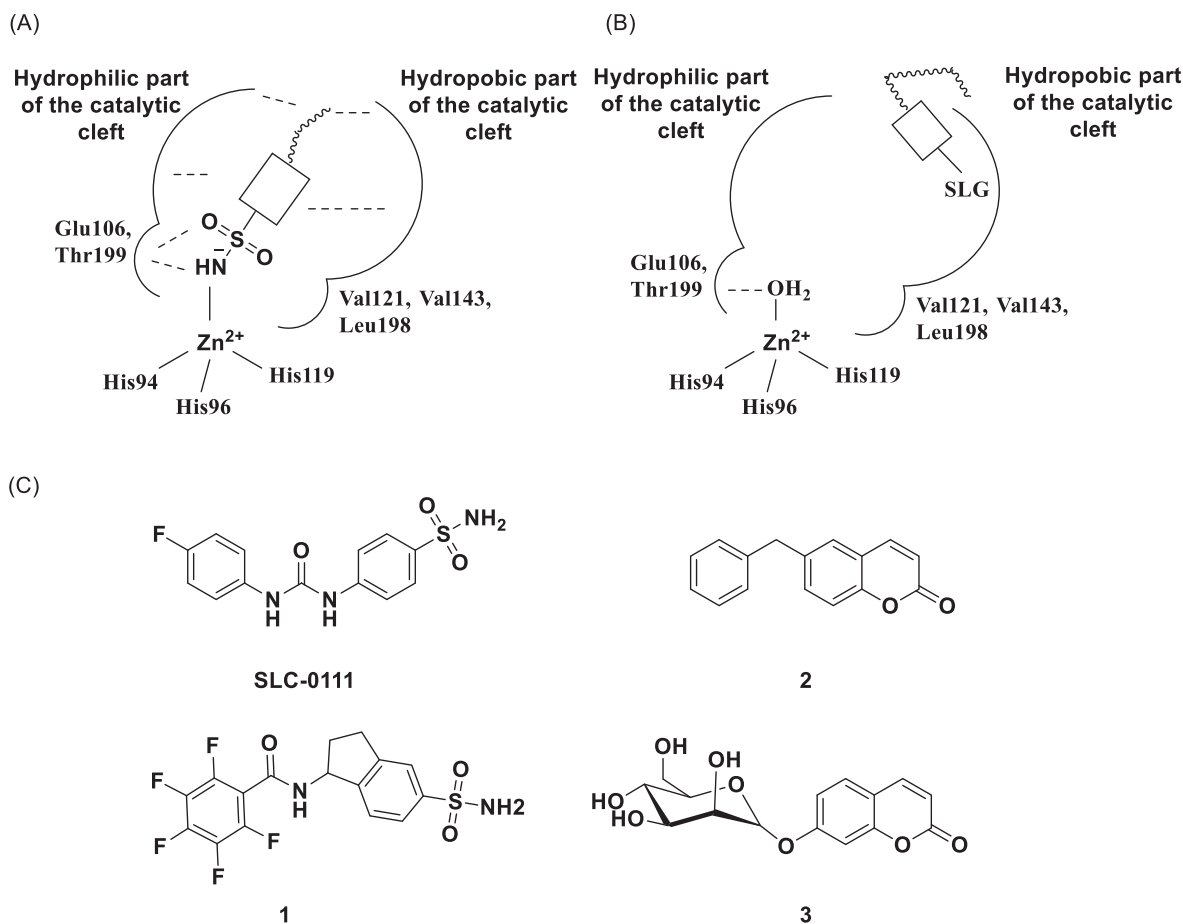


Fig. 1. (A) Schematic representation of CA inhibition via coordination to the catalytic Zn^{2+} ion. ZBG – zinc binding group. Reproduced from [33]. (B) Schematic representation of CA inhibition via occlusion of the catalytic site entrance; SLG – Sticky Lipophilic Group [33]. (C) Examples of highly potent and selective sulfonamide and coumarin based hCA IX/XII inhibitors described in literature [37,41,42].

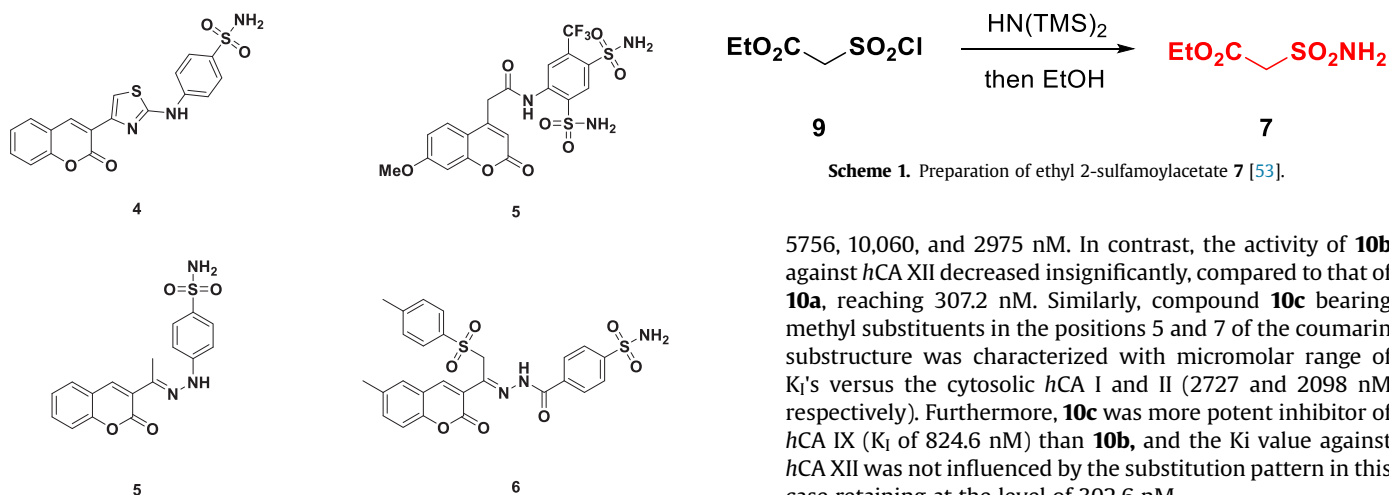
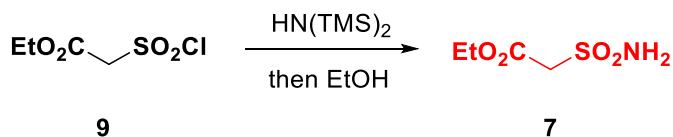


Fig. 2. Recently reported chimeric molecules **4–8** incorporating both primary sulfonamide and coumarin warheads, and their inhibition of hCA IX/XII [43–45].

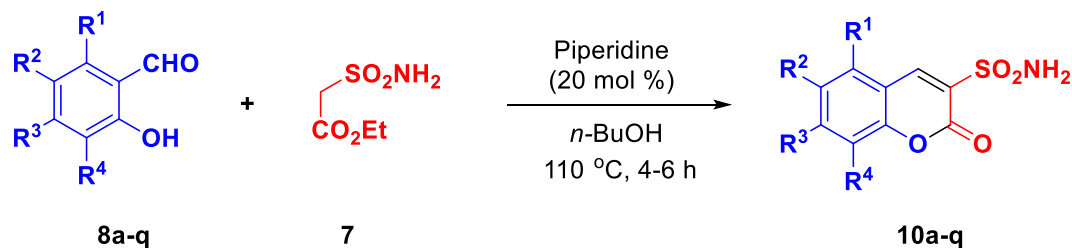
towards hCA IX characterized by K_i of 65.1 nM. Interestingly, introduction of a methoxy group into the position 5 of the coumarin scaffold caused dramatic drop in the affinities to hCA I, II and especially IX. Actually, the K_i values of the derivative **10b** towards the latter isozymes corresponded to



Scheme 1. Preparation of ethyl 2-sulfamoylacetate **7** [53].

5756, 10,060, and 2975 nM. In contrast, the activity of **10b** against hCA XII decreased insignificantly, compared to that of **10a**, reaching 307.2 nM. Similarly, compound **10c** bearing methyl substituents in the positions 5 and 7 of the coumarin substructure was characterized with micromolar range of K_i 's versus the cytosolic hCA I and II (2727 and 2098 nM respectively). Furthermore, **10c** was more potent inhibitor of hCA IX (K_i of 824.6 nM) than **10b**, and the K_i value against hCA XII was not influenced by the substitution pattern in this case retaining at the level of 302.6 nM.

- (ii) In contrast to the discussed derivatives **10b** and **10c**, 6-substituted 3-sulfamoylcoumarins **10d–j** displayed pronounced activity versus tumor-associated hCA IX and XII isozymes and some representatives showed selectivity over the cytosolic hCA I and II. Thus, both 5-methoxy- and 5-methyl substituted derivatives **10d** and **10e** exerted potent inhibition towards hCA IX and XII with K_i 's ranging between 47.3 and 77.4 nM. On the other hand, hCA I and II isoforms were only blocked at submicromolar concentrations



8a, 10a: R¹ = H, R² = H, R³ = H, R⁴ = H (80%); **8b, 10b:** R¹ = OMe, R² = H, R³ = H, R⁴ = H (54%)
8c, 10c: R¹ = Me, R² = H, R³ = Me, R⁴ = H (59%); **8d, 10d:** R¹ = H, R² = OMe, R³ = H, R⁴ = H (84%)
8e, 10e: R¹ = H, R² = Me, R³ = H, R⁴ = H (68%); **8f, 10f:** R¹ = H, R² = OH, R³ = H, R⁴ = H (75%)
8g, 10g: R¹ = H, R² = F, R³ = H, R⁴ = H (75%); **8h, 10h:** R¹ = H, R² = Cl, R³ = H, R⁴ = H (68%)
8i, 10i: R¹ = H, R² = Br, R³ = H, R⁴ = H (67%); **8j, 10j:** R¹ = H, R² = H, R³ = H, R⁴ = H (80%)
8k, 10k: R¹ = H, R² = Cl, R³ = H, R⁴ = Cl (30%); **8l, 10l:** R¹ = H, R² = H, R³ = OMe, R⁴ = H (61%)
8m, 10m: R¹ = H, R² = H, R³ = H, R⁴ = F (72%); **8n, 10n:** R¹ = H, R² = H, R³ = H, R⁴ = OH (69%)
8o, 10o: R¹ = H, R² = H, R³ = H, R⁴ = OMe (74%); **8p, 10p:** R¹ = H, R² = H, R³ = H, R⁴ = OEt (62%)
8q, 10q: R¹, R² = -(CH=CH-CH=CH-), R³ = H, R⁴ = H (33%).

Scheme 2. Synthesis of 3-sulfamoylcoumarins **10a-q** via treatment of salicylaldehydes **8a-q** with ethyl 2-sulfamoylacetate **7**.

Table 1

Inhibitory profiles compounds **10a-q** against *hCA* isoforms *hCA* I, II, IX and XII. Acetazolamide (**AAZ**) was employed as standard drug.

| N ^o | R ¹ | R ² | R ³ | R ⁴ | K _i (nM)* | | | |
|----------------|----------------|-----------------|----------------|----------------|----------------------|---------|-------|--------|
| | | | | | CA I | CA II | CA IX | CA XII |
| 10a | H | H | H | H | 481.6 | 232.4 | 65.1 | 137.5 |
| 10b | OMe | H | H | H | 5756 | 10,060 | 2975 | 307.2 |
| 10c | Me | H | Me | H | 2727 | 2098 | 824.6 | 302.6 |
| 10d | H | OMe | H | H | 543.0 | 114.8 | 58.1 | 54.4 |
| 10e | H | Me | H | H | 835.1 | 149.9 | 47.4 | 77.4 |
| 10f | H | OH | H | H | 238.5 | 53.9 | 66.4 | 26.5 |
| 10g | H | F | H | H | 257.8 | 96.7 | 32.6 | 35.8 |
| 10h | H | Cl | H | H | 920.9 | 618.1 | 176.9 | 127.9 |
| 10i | H | Br | H | H | 1450 | 1588 | 317.1 | 266.2 |
| 10j | H | NO ₂ | H | H | 946.9 | 414.1 | 147.7 | 100.7 |
| 10k | H | Cl | H | Cl | 1406 | 1249 | 518.2 | 253.6 |
| 10l | H | H | OMe | H | 330.2 | 63.1 | 40.5 | 53.8 |
| 10m | H | H | H | F | 167.5 | 69.4 | 41.1 | 26.6 |
| 10n | H | H | H | OH | 725.1 | 155.2 | 98.7 | 64.8 |
| 10o | H | H | H | OMe | 258.5 | 85.4 | 87.9 | 39.7 |
| 10p | H | H | H | OEt | 398.4 | 93.4 | 51.5 | 94.5 |
| 10q | ** | ** | H | H | 75,100 | >100 μM | 6371 | 7990 |
| AAZ | — | — | — | — | 250 | 12.5 | 25 | 5.7 |

*Mean from 3 different assays, by a stopped flow technique (errors were in the range of ± 5–10% of the reported values). ** R¹, R² = -(CH=CH-CH=CH-).

between 114.8 and 835.1 nM by **10d** and **10e** and hence certain level of isoform-selectivity was observed for these molecules. It is worth mentioning that the introduction of hydroxyl group (**10f**) or fluorine atom (**10g**) at the position 6 of the coumarin scaffold furnished the derivatives possessing equipotent double-digit nanomolar activity against *hCA* II, IX and XII isoforms. It was only *hCA* I which was slightly less sensitive to **10f,g** with K_i values of 238.5 and 257.8 nM respectively. Noticeably, replacing fluorine atom with larger halogens, such as chlorine (**10h**) and bromine (**10i**) clearly reduced the affinity of the corresponding counterparts to all

hCA isoforms in question. Indeed for **10h** K_i values for against the selected panel of enzymes ranged between 127.9 and 920.9 nM, whereas for **10i** the interval was between 266.2 and 1588 nM. However, both compounds displayed selectivity towards *hCA* IX and XII over the cytosolic isozymes. The inhibitory profile of the 6-nitro- derivative **10j** was very close to that of chlorine bearing analog **10i**. In the meantime, 6,8-dichloro-3-sulfamoylcoumarin **10k** showed micromolar activities against *hCA* I and II, while being nearly one order of magnitude more potent inhibitor of *hCA* IX and XII.

- (iii) Compound **10l** bearing methoxy group in the position 7 of the coumarin substructure exhibited significant potency against *hCA* II, IX and XII (K_i values between 40.5 and 63.1 nM) while being somewhat less active with regards to *hCA* I (K_i of 330.2). Likewise, 8-substituted derivative **10m-p** generally showed double-digit nanomolar potencies against *hCA* II, IX and XII, whereas *hCA* I was affected at concentrations spanning the range between 167.5 and 725 nM. Of this latter subset 8-fluorosubstituted analog **10m** showed the lowest K_i values against *hCA* IX and XII, namely 41.1 and 26.6 nM. Of note, contrary to compounds **10f,g**, fluoro- and hydroxysubstituted counterparts **10m** and **10n** did not possess substantial similarity in their inhibitory profiles, as **10m** was at least two times more potent against all employed isozymes.
- (iv) Finally, the investigation of the naphthalene derivative **10q** revealed that incorporation of extra aromatic rings may be detrimental for the anti-*hCA* activity of 3-sulfamoylcoumarins as it showed only micromolar K_i values against all studied enzyme isoforms.
- (v) As can be seen from Table 1, all the synthesized compounds possess moderate or weak inhibitory activity against the cytosolic isoform *hCA* I. Thus, compounds **10b**, **10c**, **10i**, **10k** and **10q** displayed only micromolar affinity to this isozyme, whereas other representatives showed submicromolar K_i values. The most potent *hCA* I inhibitor turned out to be 8-fluorosubstituted **10m** with K_i 167.5 nM. In the context of therapeutic applications of CAIs, such as anticancer or anti-glaucoma action, inhibition of *hCA* I is considered undesired, as it causes a range of unpleasant side-effects [52,58]. Therefore, the observed modest affinity of the generated molecules toward this enzyme can be deemed beneficial for their medicinal potential.
- (vi) On the other hand, the physiologically dominant *hCA* II turned out to be rather sensitive to the 3-sulfamoylcoumarins **10a-q**. Interestingly, as evident from the assay results, the presence of bulky substituents in positions 5 or 6 of the coumarin scaffold was unfavorable for the *hCA* II inhibition. In fact, compound **10b**, **10i**, and **10q** showed neglectable activity toward this enzyme. In contrast the introduction of small polar substituents in the position 6 (hydroxyl group for **10f** or fluorine atom for **10g**) significantly enhanced the *hCA* II blocking effect of the compounds as compared to the parent structure **10a**. The same was true for the 7- and 8-substituted counterparts **10l-p**, which showed *hCA* II inhibition in double-digit nanomolar range of concentrations with exception of **10n** possessing K_i as high as 155.2 nM.
- (vii) In the meantime, two tumor-associated *hCA* isoforms, namely *hCA* IX and XII were significantly affected by many of the prepared substances. Particularly, compounds **10a**, **10d**, **10e**, **10g**, and **10l-p** exerted double-digit nanomolar K_i values against *hCA* IX, being nearly equipotent to the reference drug AAZ. Similarly to *hCA* II, *hCA* IX turned out to be rather sensitive to the presence of substituents in the position 5 and 6 of the coumarin scaffold, as can be exemplified by the decreased activities of **10b**, **10c**, **10h**, **10h-k**, and especially **10q**. Interestingly, the compounds' potencies against another transmembrane isoform, *hCA* XII were remarkably close to those displayed versus *hCA* IX. Thus, with exception of **10a,b**, K_i values against these two isoforms were in the same orders of magnitude. Finally, two front running inhibitors stood out with respect to *hCA* XII, **10f** and **10m** showing K_i values of 26.5 nM. In turn, molecules **10a-c**, **10i-k** exhibited submicromolar activities whereas **10q** was ineffective versus

hCA XII just as against *hCA* IX. Therefore many of synthesized 3-sulfamoylcoumarins exerted considerable activities towards *hCA* II and more importantly against tumor-associated *hCA* IX/XII with some derivatives proved selective inhibitors of these latter isozymes.

2.3. Antiproliferative activity against cancer and normal cell lines

Development of highly potent and selective *hCA* inhibitors holds a great promise in the fields of diagnostic and management of solid tumors [59]. In fact, hostile tumor microenvironment endowed with hypoxia (due to the poor and chaotic vascularization) and acidosis (associated with glycolytic metabolism) gives rise to massive molecular and phenotypic changes and results into selection of highly aggressive types of malignant cells [60]. It has been shown, that cancer cell survival and proliferation is largely ensured by upregulation of exofacial *hCA* IX and *hCA* XII isoforms [61,62]. Not only these proteins impact significantly into pH regulation across the plasma membrane via facilitating CO₂ interconversion, but also enhance the functioning of a wide range of transport proteins [13]. Additionally, the contribution of these enzymes into pH_i and pH_e maintenance is considered crucial in disrupting intercellular adhesion contacts ensuring cancer cell invasion and metastasis [63]. However, despite the fact that several clinical studies are in progress employing well-known *hCA* inhibitors Acetazolamide (AAZ) [64,65] or SLC-0111 [66] as antiproliferative agents in combined therapy of aggressive tumors, the discovery of novel anticancer drug candidates with such mechanism is not a straightforward endeavor. This is mainly related to the frequently observed insufficient translation of *hCA* IX and XII inhibitory activities of small molecules into antiproliferative effect on cell cultures, which may have multiple reasons including compounds' off-target binding, metabolic instability, etc. [67]. Therefore, characterization and analysis of anticancer properties for the newly discovered *hCA* IX/XII inhibitors is of interest to further advance the drug discovery efforts in this field [68]. To this end the well-established MTT test in 96-well multiplate format has been performed for the synthesized compounds **10a-q**. Since, the expression of *hCA* IX in tumor cells is controlled by hypoxia-inducible factor 1 α (HIF-1 α) [13], we employed CoCl₂-induced hypoxic conditions in this study [69]. At the first stage the obtained compounds were screened in concentrations of 30, 100 and 300 μ M against the following cancer cell lines: A431 human epidermoid carcinoma, RT4 human bladder cancer, and U-87MG human glioblastoma. Additionally, Bj-5ta hTERT immortalized human foreskin fibroblasts were employed to control nonspecific cytotoxicity. The results expressed as a percentage of cells viability in comparison the control survival level (inhibitor concentration 0 μ M) set as 100% are presented in Figs. 3–6 (tabulated values can be found in Supplemental Materials, S21).

Thus, U87 MG was practically insensitive to the treatment with **10a-q**. In fact, at 30 and 100 μ M concentrations of the CAIs, no significant inhibition of cell growth was observed, and furthermore, increased proliferation rates were detected in many cases. The only two compounds that approached 50% inhibition levels at 300 μ M concentration turned out to be **10k** and **10m** (in presence of these compounds observed cell viability amounted to 54.13 and 57.93). Of note, the *hCA* IX/XII inhibitory activities of these hit compounds differed significantly, as **10m** was one of the most potent agent against these isozymes (K_i 's of 41.1 and 26.6 nM respectively), whereas **10k** displayed one order of magnitude lower K_i values (518.2 and 253.6 nM correspondingly). In addition, compounds **10n** and **10q** exerted decreased U87 MG cell survival rates to ca. 70% levels (more precisely 67.7 and 67.92) at 300 μ M concentrations.

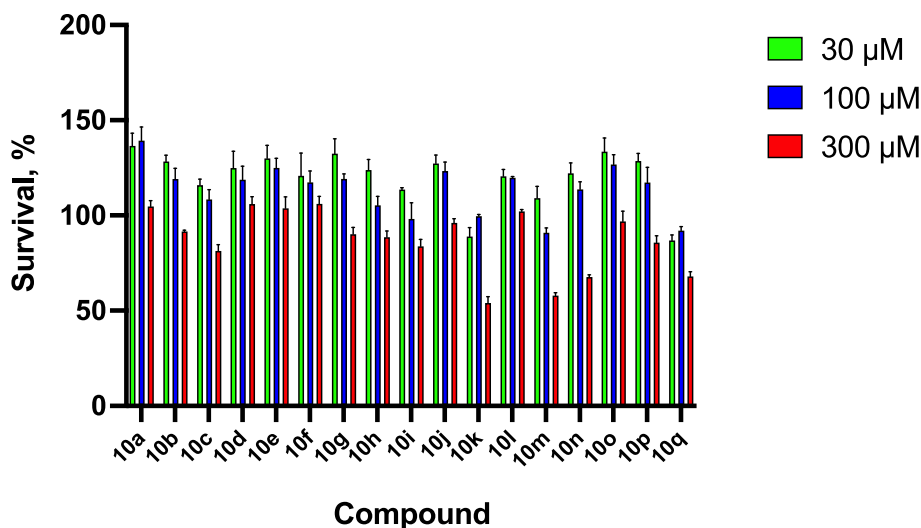


Fig. 3. Cell viability MTT assay results for compounds **10a-q** at 30 (green), 100 (blue) and 300 (red) μM concentrations against U-87MG cell line under hypoxic conditions (100 μM CoCl₂). Values are displayed in % as the mean ± SEM of three experiments relative to control (0 μM, 100% viability, not shown).

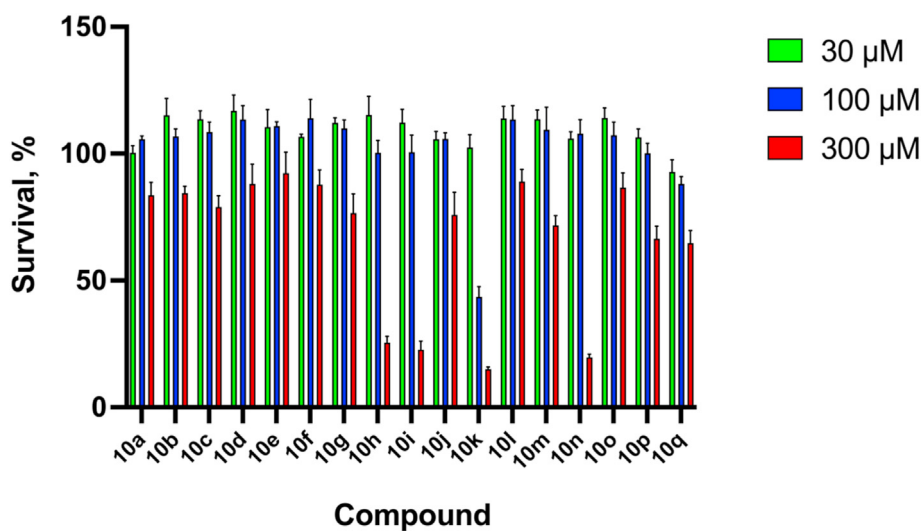


Fig. 4. Cell viability MTT assay results for compounds **10a-q** at 30 (green), 100 (blue) and 300 (red) μM concentrations against RT4 cell line under hypoxic conditions (100 μM CoCl₂). Values are displayed in % as the mean ± SEM of three experiments relative to control (0 μM, 100% viability, not shown).

Again, while **10n** was rather potent *hCA* IX/XII inhibitor (K_i values of 98.6 and 64.8), **10q** was the least active blocker of these isoforms with respect to all tested compounds (K_i values of 6371 and 7990 nM). Therefore, despite 3-sulfamoyl coumarins **10a-q** showed U87 MG growth suppressing effect, if any, only at very high concentrations, the results highlighted the fact that *hCA* IX/XII inhibition may not be the only mechanism of the observed antiproliferative effect, as *hCA* inhibitory profiles of the hit compounds were polar opposite to each other.

Unlike U-87 MG, RT-4 cell line exhibited more pronounced response when treated with 3-sulfamoylcoumarins **10a-q**. Indeed, at least one compound **10k** displayed clear dose-dependent antiproliferative effect on this cell culture with 43.54 and 15.05% cell viability levels at 100 and 300 μM concentrations respectively. As discussed above **10k** demonstrated potent inhibition of *hCA* IX and XII and therefore its anticancer effect could be at least partially related to the blocking of *hCA* enzymatic activity. Compounds **10h**, **10i** and **10n**, in turn, influenced RT-4 cell growth at 300 μM (cell

viability levels ranged between 19.70 and 25.42%), yet their antiproliferative effect was not observed at lower concentration ranges.

Of all examined cancer cell lines A431 cells turned out to be the most sensitive to the compounds **10a-q**. To our delight, four derivatives **10h**, **10i**, **10k** and **10q** exerted profound antiproliferative effect on these cells. Intriguingly, as in the case of RT-4 potent *hCA* IX/XII inhibitor **10k** caused distinct response with cell survival rates of 38.76 and 2.84% at 100 and 300 μM concentrations respectively. On the other hand, derivatives **10h** and **10i** possessing sub-micromolar K_i values against the tumor-associated *hCA* isoforms exhibited nearly identical levels of A431 cell survival at all three tested concentrations (e.g. 36.48 and 39.33% at 300 μM concentrations correspondingly). Meanwhile, **10q** that was found inactive versus *hCA* IX and XII isoforms also showed marked effect on the A431 cell growth with percentage of living cells of 72.95 and 23.41 at 100 and 300 μM concentrations.

With a view to control nonspecific cytotoxicity of the synthesized compounds **10a-q**, their effect on the growth of normal

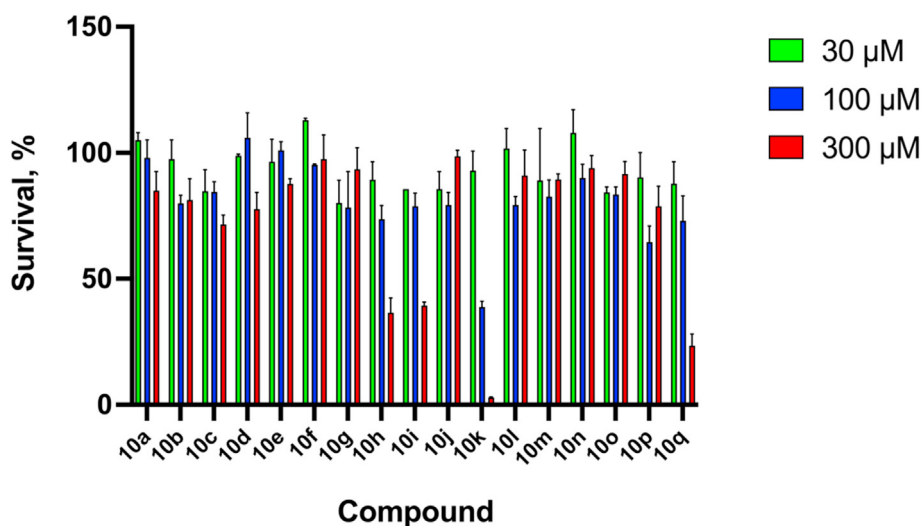


Fig. 5. Cell viability MTT assay results for compounds **10a-q** at 30 (green), 100 (blue) and 300 (red) μM concentrations against A431 cell line under hypoxic conditions (100 μM CoCl_2). Values are displayed in % as the mean \pm SEM of three experiments relative to control (0 μM , 100% viability, not shown).

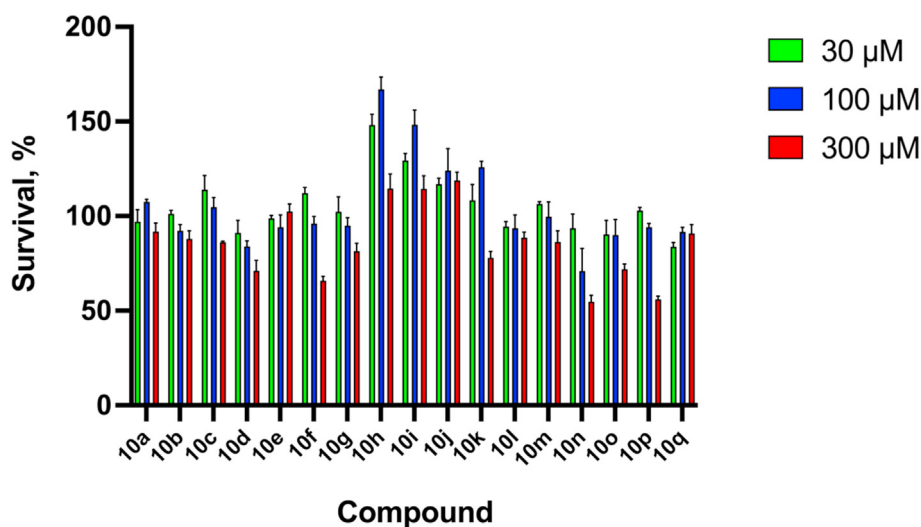


Fig. 6. Cell viability MTT assay results for compounds **10a-q** at 30 (green), 100 (blue) and 300 (red) μM concentrations against Bj-5ta hTERT cell culture under hypoxic conditions (100 μM CoCl_2). Values are displayed in % as the mean \pm SEM of three experiments relative to control (0 μM , 100% viability, not shown).

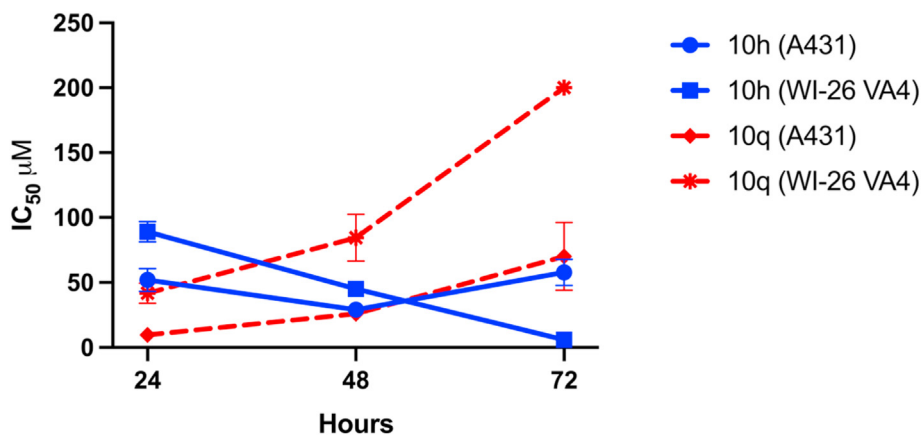
human cells has been evaluated. Specifically, Bj-5ta hTERT immortalized human foreskin fibroblasts have been employed for this purpose. Reassuringly, derivatives **10a-q** were generally well tolerated by Bj-5ta cells, which were only sensitive to at 300 μM concentrations of **10d** (cell viability 70.97%), **10f** (65.75%), **10n** (54.76%) and **10p** (55.97). It is important to note that the front running compounds **10h**, **10i**, **10k** and **10q** exhibiting remarkable antiproliferative activity against malignant cell lines (*vide supra*) did not show any detectable effect on the survival of healthy human cells. The latter observation renders these agents attractive in terms of more detailed investigation of their anticancer properties.

In order to further characterize the anticancer activity of the four discovered hit compounds **10h**, **10i**, **10k** and **10q** we proceeded to determine their IC_{50} values. To this end, dose-response curves have been obtained against the most sensitive A431 cancer cell line (Supplementary materials, S22-25). Moreover, since A341 cells originate from human lungs, WI-26 AV4 healthy human lung fibroblasts cell culture was employed as a control in this experiment (Table 2).

As evident from Table 2 compounds **10h**, **10i** and **10k** possessed A431 IC_{50} values in double-digit micromolar range, with limited deviations observed at different incubation times. In contrast, compound **10q** displayed clearly growing IC_{50} values (from 9.73 to 70.14 μM) with increasing the incubation time. Furthermore, while pronounced cumulative effect was observed for **10h**, **10i** and **10k** against the normal WI-26 AV4 cells, **10q** showed the opposite behavior and the IC_{50} values grew consistently reaching more than 350 μM after incubating for 72 h. It is worth noting that unlike **10h**, **10i** and **10k**, naphthalene derivative **10h** exerted nearly no inhibition of tumor-associated *hCA IX* and *XII*, yet its antiproliferative properties were distinguished with a clear time- and dose-dependent character. Unexpectedly, both A431 and WI-26 AV4 cell lines demonstrated progressive desensibilization to the incubation with **10q**, which was not observed for the other tested 3-sulfamoylcoumarins. It should be additionally stressed that compound **10q** retained its selectivity toward the A431 cell line over the non-tumorigenic normal human fibroblast cell line WI-26 AV4. The latter trend is vividly illustrated in Fig. 7 representing the observed

Table 2IC₅₀ values of the hit compounds **10h**, **10i**, **10k** and **10q** as well as anticancer kinase inhibitor Gefitinib at different incubation times against A431 and WI-26 AV4 cell lines.

| Compound | A431 | | | WI-26 AV4 | | |
|------------|-----------------------|--------------|---------------|-----------------------|---------------|--------------|
| | IC ₅₀ , μM | | | IC ₅₀ , μM | | |
| | 24 h | 48 h | 72 h | 24 h | 48 h | 72 h |
| 10h | 51.91 ± 8.85 | 29.10 ± 3.57 | 57.80 ± 10.00 | 89.15 ± 7.82 | 45.11 ± 1.92 | 5.87 ± 1.69 |
| 10i | 38.43 ± 5.60 | 24.7 ± 3.99 | 49.20 ± 9.63 | 76.57 ± 7.13 | 42.05 ± 2.08 | 21.5 ± 2.48 |
| 10k | 26.89 ± 4.36 | 20.30 ± 1.91 | 35.24 ± 3.40 | 73.97 ± 30.04 | 9.54 ± 1.03 | 14.35 ± 1.70 |
| 10q | 9.73 ± 3.13 | 25.91 ± 5.86 | 70.14 ± 26.06 | 41.68 ± 7.84 | 84.48 ± 17.92 | >350 |
| Gefitinib | 32.17 ± 3.44 | 24.55 ± 2.58 | 16.02 ± 2.87 | 51.18 ± 7.44 | 42.95 ± 6.55 | 38.76 ± 4.37 |

**Fig. 7.** Shifts in IC₅₀ values at increasing incubation times for compounds **10h** and **10q** against A431 and WI-26 AV cells.

shifts in the IC₅₀ values for **10h** and **10q** against the said cell lines.

Such strikingly different modes of action for **10q** and the remaining hit compounds could be hypothetically related to differing mechanisms of the observed anticancer effects exerted by these compounds. In fact, as the only compound in the set based on the planar 2*H*-benzo [*h*]chromen-2-one nucleus, **10q** could potentially bind a wide range of essential biomolecules, including DNA, which is unlikely the case for the other obtained compounds bearing low-bulk non-cyclic substituents at their coumarin cores. Being structurally similar to polycyclic aromatic hydrocarbon DNA intercalators [70–72], should **10q** exert genotoxicity and induce apoptosis, which is typical for classical DNA-intercalating chemotherapeutics [73].

2.4. Apoptosis detection by Annexin V-FITC and caspase 3/7 assays

Apoptosis, a physiological process of programmed cell death, is disrupted in malignant cells [74]. Hence, apoptosis induction by various chemotherapeutic agents has been widely exploited in the context of cancer treatment [75]. Noticeably, sulfonamide based *hCA* inhibitors are known to possess cytotoxic effect to malignant cells by inducing apoptosis [76,77]. The same is true for a range of recently reported sulfonamide bearing coumarins for which the mechanism of anticancer action remains unraveled [78,79]. In this context, Annexin V-FITC/propidium iodide (AV/PI) dual staining assay was performed to examine the impact of 3-sulfamoylcoumarin **10q** in 5–25 μM concentrations on early and late apoptosis levels in A431 cells (Fig. 8). The obtained morphological data indicated that treatment of A431 cells with 25 μM **10q** resulted into a substantial increase in the percent of Annexin V-FITC-positive early apoptotic cells from 6.10% to 18.56% after 24 h incubation which corresponds to 3-fold total increase as compared to control. In the meantime, the fraction of late apoptotic cells

slightly decreased under the same conditions from 3.06% to 2.31%, and the percentage of dead cells grew from 0.14% to 0.41%. Thereby, dose-dependent induction of apoptosis was displayed by compound **10q** after incubation with A431 cancer cells (Fig. 8).

Apoptosis is known to be a highly regulated and controlled biochemical process associated with caspase enzyme activity [80]. To further establish the cell death pathway induced by **10q** the activation of caspases 3/7 was evaluated. Expectedly, in a full accordance with the obtained morphological data, dose-dependent caspase 3/7 activation was vividly displayed by the compound **10q** as can be seen from Fig. 9 (Fig. 9).

In this manner the results of the study showed that apoptosis was promoted by compound **10q** through mediation of caspases in the A431 cells.

3. Conclusion

In summary, *hCA* IX and XII are promising therapeutic targets with regards to management of hypoxic solid tumors. A range of primary sulfonamide and coumarin based inhibitors display remarkable potency and isoform-selectivity toward these isozymes. We have designed and synthesized a novel type of chimeric molecules comprising primary sulfonamide group directly attached to the coumarin core at its 3 position. The synthesis was performed via introduction of ethyl 2-sulfamoylacetate into Knoevenagel condensation with diversely substituted salicylaldehydes, furnishing target molecules in moderate to high yields. Inhibitory profiles of seventeen newly synthesized compounds against a panel of four physiologically relevant *hCA* isoforms (*hCA* I, II, IX and XII) have been determined. Noticeably, the obtained molecules were generally potent *hCA* inhibitors, with many compounds possessing K_i values in double-digit nanomolar range. Encouragingly, tumor-associated isoforms *hCA* IX and XII were significantly affected by

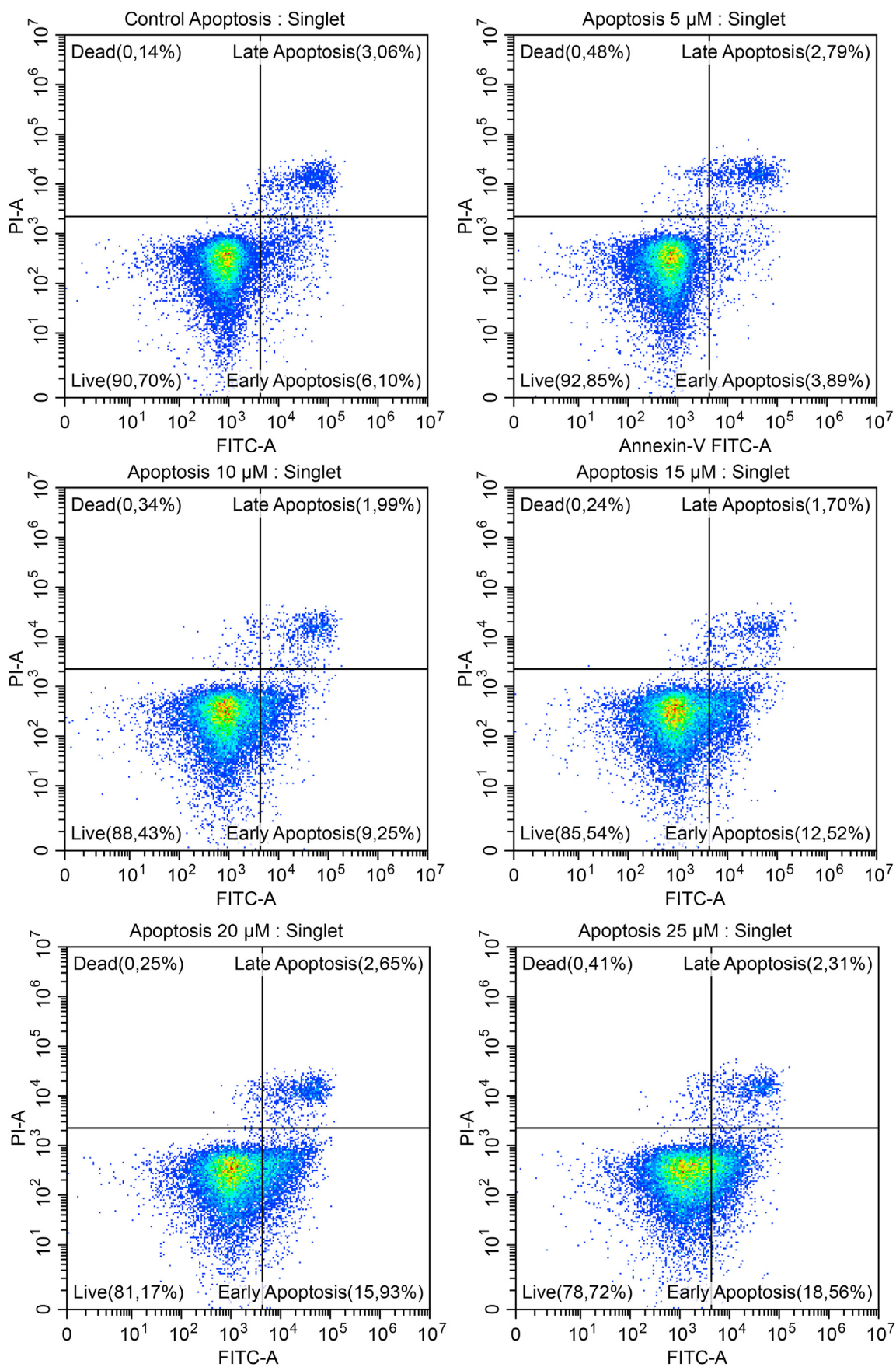


Fig. 8. Apoptosis induction caused by different concentrations of hit compound 10q against A431 cell line.

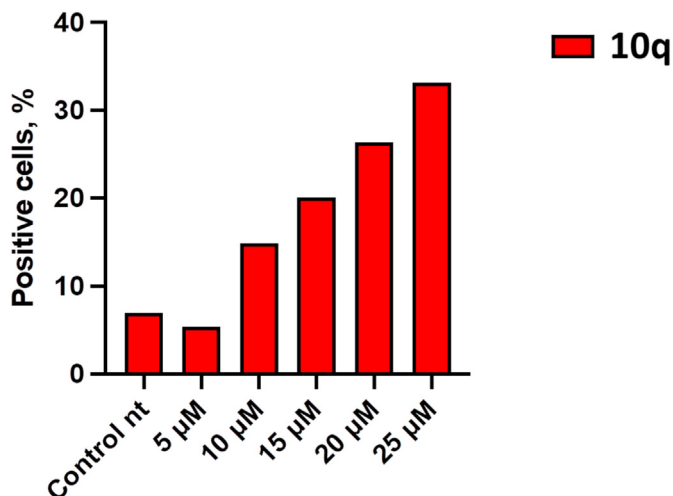


Fig. 9. Caspase 3/7 activation exerted by **10q** after incubation with A431 cells for 24 h at different concentrations.

several hit compounds displaying selectivity over the widespread cytosolic *hCA* II. In addition, weak inhibition was exerted towards another cytosolic isozyme *hCA* I which is considered an off-target protein for the therapeutically relevant *hCA* inhibitors. In this context, antiproliferative effect of the obtained compounds has been measured against three human cancer cell lines and one non-tumorigenic healthy human cell line under hypoxic conditions. Thus, while, U-87MG human glioblastoma cells were insensitive to the treatment with the synthesized 3-sulfamoylcoumarins, RT4 human bladder cancer and especially A431 human epidermoid carcinoma cells were efficiently inhibited by several newly obtained derivatives in a dose-dependent manner. In fact, four hit compounds **10h**, **10i**, **10k**, and **10q** have been discovered displaying low nanomolar IC_{50} values against A431 cell line. Unexpectedly, the behavior of the most potent and selective antiproliferative agent **10q** turned out to drastically differ from the remaining hits. Thus, nearly 10-fold shifts in IC_{50} values was observed for **10q** at 24 and 72 incubation times, against both cancer and non-tumorigenic human cells. Consequently, **10q** was characterized as potent cytotoxic agent inducing apoptosis in A431 cells. Furthermore, dose-dependent caspase 3/7 activation has been shown in presence of this compound. Thus, as contrasted to *hCA* inhibitory compounds **10h**, **10i**, **10k** which displayed poorly selective anticancer profile, **10q** devoid of *hCA* IX/XII blocking activity, exhibited selective time- and dose-dependent cytotoxic properties against A431 cell culture. The mechanism of the observed cytotoxic effect requires further investigation which will be reported in due course.

4. Experimental section

4.1. General experimental procedures

All commercial reagents were used without purification. NMR spectrum were recorded using Bruker Avance III spectrometer in DMSO- d_6 (1H : 400.13 MHz; ^{13}C : 100.61 MHz; ^{19}F : 376.50 MHz); chemical shifts are reported as parts per million (δ , ppm); the residual solvent peak was used as internal standard: 2.50 ppm for 1H , 39.52 ppm for ^{13}C ; multiplicities are abbreviated as follows: s = singlet, d = doublet, t = triplet, q = quartet, m = multiplet, br = broad, dd = doublet of doublets, dt = doublet of triplets; coupling constants, J , are reported in Hz. Mass spectrum were recorded using Bruker microTOF spectrometer (ionization by electrospray, positive ions detection). Melting points were

determined in open capillary tubes on Stuart SMP50 Automatic Melting Point Apparatus. Analytical thin-layer chromatography was carried out on UV-254 silica gel plates using appropriate eluents. Compounds were visualized with short-wavelength UV light.

4.1.1. Preparation of ethyl 2-sulfamoylacetate (**11**) [53]

To a solution of ethyl 2-(chlorosulfonyl)acetate **14** [81,82] (1.87 g, 10 mmol) in dry DCM (8 mL) under ice-cooling was slowly added hexamethyldisilazane (2.2 mL, 10.5 mmol). Mixture was stirred under cooling for 30 min, and then 30 min without bath. Solvent was removed *in vacuo*. The oily residue was cooled in ice bath, dissolved in ethanol (5 mL), and stirred for 45 min. Evaporation of solvent gave white solid, 1.35 g (81%). 1H NMR (400 MHz, $CDCl_3$) δ 5.25 (br.s, 2H), 4.31 (q, $J = 7.2$ Hz, 2H), 4.14 (s, 2H), 1.35 (t, $J = 7.1$ Hz, 3H).

4.1.2. General procedure for the preparation of sulfamoyl coumarins **10a-q**

A mixture of ethyl 2-sulfamoylacetate (**10a-q**) (167 mg, 1.0 mmol) and corresponding salicylaldehyde (1.0 mmol) in *n*-butanol (2 mL) was stirred in a closed vessel at 110 °C for 2–6 h (controlled by TLC). Upon cooling to ambient temperature, the precipitate was collected, washed with ether (3×1.5 mL) and dried *in vacuo* to afford the target coumarins **10a-q**.

4.1.2.1. 2-Oxo-2H-chromene-3-sulfonamide (10a). Prepared from salicylaldehyde according to the general procedure; yield: 181 mg (80%). White solid; m. p. 255.1–256.5 °C. 1H NMR (400 MHz, DMSO- d_6) δ 8.75 (s, 1H), 8.01 (dd, $J = 7.8, 1.6$ Hz, 1H), 7.77 (dd, $J = 8.7, 7.3, 1.6$ Hz, 1H), 7.51 (d, $J = 7.8$ Hz, 1H), 7.50 (br.s, 2H), 7.46 (td, $J = 7.5, 1.0$ Hz, 1H). $^{13}C\{^1H\}$ NMR (101 MHz, DMSO- d_6) δ 155.8, 154.6, 144.7, 134.9, 131.1, 129.9, 125.7, 117.9, 116.8. HRMS (ESI), m/z calcd for $C_9H_7NNaO_4S$ [$M+Na$] $^+$ 247.9988 found 247.9993.

4.1.2.2. 5-Methoxy-2-oxo-2H-chromene-3-sulfonamide (10 b). Prepared from 6-methoxysalicylaldehyde according to the general procedure; yield: 138 mg (54%). White solid; m. p. 250.6–251.4 °C. 1H NMR (400 MHz, DMSO- d_6) δ 8.61 (d, $J = 0.7$ Hz, 1H), 7.73 (t, $J = 8.4$ Hz, 1H), 7.51 (br.s, 2H), 7.09–7.03 (m, 2H), 3.99 (s, 3H). $^{13}C\{^1H\}$ NMR (101 MHz, DMSO- d_6) δ 157.6, 155.6, 155.5, 138.8, 136.3, 128.2, 108.9, 107.9, 107.3, 57.1. HRMS (ESI), m/z calcd for $C_{10}H_9NNaO_5S$ [$M+Na$] $^+$ 278.0094 found 278.0094.

4.1.2.3. 5,7-Dimethyl-2-oxo-2H-chromene-3-sulfonamide (10c). Prepared from 4,6-dimethylsalicylaldehyde according to the general procedure; yield: 149 mg (59%). White solid; m. p. 227.9–229.8 °C. 1H NMR (400 MHz, DMSO- d_6) δ 8.55 (s, 1H), 7.49 (br.s, 2H), 7.17 (s, 1H), 7.15 (s, 1H), 2.53 (s, 3H), 2.41 (s, 3H). $^{13}C\{^1H\}$ NMR (101 MHz, DMSO- d_6) δ 155.8, 155.4, 146.2, 141.2, 138.8, 128.1, 128.0, 114.8, 114.1, 21.9, 18.2. HRMS (ESI), m/z calcd for $C_{11}H_{11}NNaO_4S$ [$M+Na$] $^+$ 276.0301 found 276.0304.

4.1.2.4. 6-Methoxy-2-oxo-2H-chromene-3-sulfonamide (10 d). Prepared from 5-methoxysalicylaldehyde according to the general procedure; yield: 214 mg (84%). Pale yellow solid; m. p. 242.4–243.6 °C. 1H NMR (400 MHz, DMSO- d_6) δ 8.70 (s, 1H), 7.60 (d, $J = 3.0$ Hz, 1H), 7.50 (br.s, 2H), 7.46 (d, $J = 9.1$ Hz, 1H), 7.36 (dd, $J = 9.1, 3.0$ Hz, 1H), 3.83 (s, 3H). $^{13}C\{^1H\}$ NMR (101 MHz, DMSO- d_6) δ 156.4, 156.0, 149.0, 144.5, 130.1, 122.5, 118.3, 117.9, 112.9, 56.3. HRMS (ESI), m/z calcd for $C_{10}H_9NNaO_5S$ [$M+Na$] $^+$ 278.0094 found 278.0098.

4.1.2.5. 6-Methyl-2-oxo-2H-chromene-3-sulfonamide (10e). Prepared from 5-methylsalicylaldehyde according to the general procedure; yield: 163 mg (68%). White solid; m. p. 240.5–243.6 °C.

^1H NMR (400 MHz, DMSO- d_6) δ 8.65 (s, 1H), 7.77 (d, J = 2.1 Hz, 1H), 7.57 (dd, J = 8.5, 2.2 Hz, 1H), 7.50 (br.s, 2H), 7.39 (d, J = 8.5 Hz, 1H), 2.38 (s, 3H). $^{13}\text{C}\{^1\text{H}\}$ NMR (101 MHz, DMSO- d_6) δ 156.0, 152.8, 144.5, 135.8, 135.1, 130.4, 129.8, 117.5, 116.5, 20.7. HRMS (ESI), m/z calcd for $\text{C}_{10}\text{H}_9\text{NNaO}_4\text{S}$ [$\text{M}+\text{Na}$] $^+$ 262.0145 found 262.0148.

4.1.2.6. 6-Hydroxy-2-oxo-2H-chromene-3-sulfonamide (10f).

Prepared from 5-hydroxysalicylaldehyde according to the general procedure; yield: 181 mg (75%). Beige solid; m. p. >290 °C. ^1H NMR (400 MHz, DMSO- d_6) δ 9.82 (br.s, 1H), 8.67 (s, 1H), 7.52 (br.s, 2H), 7.36 (d, J = 8.9 Hz, 1H), 7.30 (d, J = 2.9 Hz, 1H), 7.19 (dd, J = 9.0, 2.9 Hz, 1H). $^{13}\text{C}\{^1\text{H}\}$ NMR (101 MHz, DMSO- d_6) δ 156.1, 154.7, 148.0, 144.7, 129.8, 123.0, 118.4, 117.7, 114.7. HRMS (ESI), m/z calcd for $\text{C}_9\text{H}_7\text{NNaO}_5\text{S}$ [$\text{M}+\text{Na}$] $^+$ 263.9937 found 263.9941.

4.1.2.7. 6-Fluoro-2-oxo-2H-chromene-3-sulfonamide (10 g).

Prepared from 5-fluorosallylaldehyde according to the general procedure; yield: 182 mg (75%). White solid; m. p. 251.8–253.0 °C. ^1H NMR (400 MHz, DMSO- d_6) δ 8.73 (s, 1H), 7.91 (dd, J = 8.4, 3.0 Hz, 1H), 7.65 (td, J = 8.9, 3.1 Hz, 1H), 7.59 (br.s, 2H), 7.57 (dd, J = 9.2, 4.5 Hz, 3H). $^{13}\text{C}\{^1\text{H}\}$ NMR (101 MHz, DMSO- d_6) δ 158.6 (d, J = 241.8 Hz), 155.6, 151.1 (d, J = 1.8 Hz), 143.8 (d, J = 2.9 Hz), 130.8, 122.2 (d, J = 24.9 Hz), 118.9 (d, J = 8.7 Hz), 118.8 (d, J = 10.0 Hz), 116.0 (d, J = 24.6 Hz). $^{19}\text{F}\{^1\text{H}\}$ NMR (376 MHz, DMSO- d_6) δ -116.92. HRMS (ESI), m/z calcd for $\text{C}_9\text{H}_6\text{FNNaO}_4\text{S}$ [$\text{M}+\text{Na}$] $^+$ 265.9894 found 265.9896.

4.1.2.8. 6-Chloro-2-oxo-2H-chromene-3-sulfonamide (10 h).

Prepared from 5-chlorosalicylaldehyde according to the general procedure; yield: 177 mg (68%). White solid; m. p. 271.2–272.3 °C. ^1H NMR (400 MHz, DMSO- d_6) δ 8.73 (s, 1H), 8.15 (d, J = 2.6 Hz, 1H), 7.80 (dd, J = 8.9, 2.6 Hz, 1H), 7.57 (br.s, 2H), 7.55 (d, J = 8.9 Hz, 1H). $^{13}\text{C}\{^1\text{H}\}$ NMR (101 MHz, DMSO- d_6) δ 155.5, 153.3, 143.5, 134.3, 130.9, 129.9, 129.3, 119.3, 118.8. HRMS (ESI), m/z calcd for $\text{C}_9\text{H}_6\text{ClNNaO}_4\text{S}$ [$\text{M}+\text{Na}$] $^+$ 281.9598 found 281.9599.

4.1.2.9. 6-Bromo-2-oxo-2H-chromene-3-sulfonamide (10i).

Prepared from 5-bromosalicylaldehyde according to the general procedure; yield: 204 mg (67%). Pale yellow solid; m. p. 281.8–283.6 °C (decomp.). ^1H NMR (400 MHz, DMSO- d_6) δ 8.72 (s, 1H), 8.28 (d, J = 2.4 Hz, 1H), 7.91 (dd, J = 8.9, 2.4 Hz, 1H), 7.57 (br.s, 2H), 7.48 (d, J = 8.9 Hz, 1H). $^{13}\text{C}\{^1\text{H}\}$ NMR (101 MHz, DMSO- d_6) δ 155.4, 153.7, 143.5, 137.1, 132.9, 130.9, 119.8, 119.1, 117.2. HRMS (ESI), m/z calcd for $\text{C}_9\text{H}_6\text{BrNNaO}_4\text{S}$ [$\text{M}+\text{Na}$] $^+$ 325.9093 found 325.9097.

4.1.2.10. 6-Nitro-2-oxo-2H-chromene-3-sulfonamide (10j).

Prepared from 5-nitrosallylaldehyde according to the general procedure; yield: 111 mg (41%). Beige solid; m. p. 241.4–243.6 °C. ^1H NMR (400 MHz, DMSO- d_6) δ 9.03 (d, J = 2.7 Hz, 1H), 8.94 (s, 1H), 8.53 (dd, J = 9.2, 2.8 Hz, 1H), 7.72 (d, J = 9.2 Hz, 1H), 7.65 (br.s, 2H). $^{13}\text{C}\{^1\text{H}\}$ NMR (101 MHz, DMSO- d_6) δ 158.2, 155.0, 144.4, 143.7, 131.6, 129.0, 126.9, 118.5, 118.4. HRMS (ESI), m/z calcd for $\text{C}_9\text{H}_6\text{N}_2\text{NaO}_6\text{S}$ [$\text{M}+\text{Na}$] $^+$ 292.9839 found 292.9845.

4.1.2.11. 6,8-Dichloro-2-oxo-2H-chromene-3-sulfonamide (10 k).

Prepared from 3,5-dichlorosalicylaldehyde according to the general procedure; yield: 88 mg (30%). Pale yellow solid; m. p. 217.7–218.8 °C. ^1H NMR (400 MHz, DMSO- d_6) δ 8.73 (s, 1H), 8.14 (d, J = 2.5 Hz, 1H), 8.09 (d, J = 2.3 Hz, 1H), 7.65 (br.s, 2H). $^{13}\text{C}\{^1\text{H}\}$ NMR (101 MHz, DMSO- d_6) δ 154.7, 149.2, 143.3, 133.6, 131.6, 129.2, 129.0, 121.5, 120.5. HRMS (ESI), m/z calcd for $\text{C}_9\text{H}_5\text{Cl}_2\text{NNaO}_4\text{S}$ [$\text{M}+\text{Na}$] $^+$ 315.9209 found 315.9211.

4.1.2.12. 7-Methoxy-2-oxo-2H-chromene-3-sulfonamide (10 l).

Prepared from 4-methoxysallylaldehyde according to the general

procedure; yield: 156 mg (61%). Beige solid; m. p. 191.6–193.8 °C. ^1H NMR (400 MHz, DMSO- d_6) δ 8.67 (s, 1H), 7.92 (d, J = 8.7 Hz, 1H), 7.40 (br.s, 2H), 7.11 (d, J = 2.4 Hz, 1H), 7.06 (dd, J = 8.7, 2.4 Hz, 1H), 3.91 (s, 3H). $^{13}\text{C}\{^1\text{H}\}$ NMR (101 MHz, DMSO- d_6) δ 165.0, 156.9, 156.2, 144.9, 132.3, 126.1, 114.0, 111.2, 101.1, 56.7. HRMS (ESI), m/z calcd for $\text{C}_{10}\text{H}_9\text{NNaO}_5\text{S}$ [$\text{M}+\text{Na}$] $^+$ 278.0094 found 278.0095.

4.1.2.13. 8-Fluoro-2-oxo-2H-chromene-3-sulfonamide (10 m).

Prepared from 3-fluorosallylaldehyde according to the general procedure; yield: 175 mg (72%). White solid; m. p. 262.4–263.6 °C. ^1H NMR (400 MHz, DMSO- d_6) δ 8.78 (d, J = 1.4 Hz, 1H), 7.83 (dt, J = 7.9, 1.2 Hz, 1H), 7.72 (dd, J = 10.9, 8.3, 1.4 Hz, 1H), 7.60 (br.s, 2H), 7.44 (td, J = 8.0, 4.7 Hz, 1H). $^{13}\text{C}\{^1\text{H}\}$ NMR (101 MHz, DMSO- d_6) δ 154.7, 148.7 (d, J = 248.7 Hz), 144.2 (d, J = 2.8 Hz), 142.5 (d, J = 11.5 Hz), 130.7, 126.5 (d, J = 3.7 Hz), 125.7 (d, J = 6.9 Hz), 120.8 (d, J = 16.9 Hz), 119.9. $^{19}\text{F}\{^1\text{H}\}$ NMR (376 MHz, DMSO- d_6) δ -134.80. HRMS (ESI), m/z calcd for $\text{C}_9\text{H}_6\text{FNNaO}_4\text{S}$ [$\text{M}+\text{Na}$] $^+$ 265.9894 found 265.9896.

4.1.2.14. 8-Hydroxy-2-oxo-2H-chromene-3-sulfonamide (10n).

Prepared from 3-hydroxysallylaldehyde according to the general procedure; yield: 166 mg (69%). Beige solid; m. p. >290 °C (decomp.). ^1H NMR (400 MHz, DMSO- d_6) δ 8.67 (s, 1H), 7.81 (br.s, 3H), 7.43–7.38 (m, 1H), 7.28–7.23 (m, 2H). $^{13}\text{C}\{^1\text{H}\}$ NMR (101 MHz, DMSO- d_6) δ 155.8, 145.1, 145.0, 143.2, 129.7, 125.7, 121.1, 120.8, 118.8. HRMS (ESI), m/z calcd for $\text{C}_9\text{H}_7\text{NNaO}_5\text{S}$ [$\text{M}+\text{Na}$] $^+$ 263.9937 found 263.9935.

4.1.2.15. 8-Methoxy-2-oxo-2H-chromene-3-sulfonamide (10°).

Prepared from 3-methoxysallylaldehyde according to the general procedure; yield: 189 mg (74%). White solid; m. p. 244.6–245.5 °C. ^1H NMR (400 MHz, DMSO- d_6) δ 8.71 (s, 1H), 7.54 (dd, J = 7.8, 1.5 Hz, 1H), 7.51 (br.s, 2H), 7.45 (dd, J = 8.2, 1.5 Hz, 1H), 7.38 (t, J = 7.9 Hz, 1H), 3.94 (s, 3H). $^{13}\text{C}\{^1\text{H}\}$ NMR (101 MHz, DMSO- d_6) δ 155.5, 146.8, 144.9, 143.9, 130.0, 125.7, 121.9, 118.4, 117.0, 56.7. HRMS (ESI), m/z calcd for $\text{C}_{10}\text{H}_9\text{NNaO}_5\text{S}$ [$\text{M}+\text{Na}$] $^+$ 278.0094 found 278.0097.

4.1.2.16. 8-Ethoxy-2-oxo-2H-chromene-3-sulfonamide (10p).

Prepared from 3-ethoxysallylaldehyde according to the general procedure; yield: 167 mg (62%). Pale tan solid; m. p. 178.0–179.8 °C. ^1H NMR (400 MHz, DMSO- d_6) δ 8.71 (s, 1H), 7.53 (dd, J = 7.7, 1.4 Hz, 1H), 7.51 (br.s, 2H), 7.44 (dd, J = 8.3, 1.5 Hz, 1H), 7.38–7.34 (m, 1H), 4.21 (q, J = 6.9 Hz, 2H), 1.42 (t, J = 7.0 Hz, 3H). $^{13}\text{C}\{^1\text{H}\}$ NMR (101 MHz, DMSO- d_6) δ 155.6, 146.1, 145.0, 144.0, 130.0, 125.7, 121.9, 118.5, 117.9, 65.1, 15.0. HRMS (ESI), m/z calcd for $\text{C}_{11}\text{H}_{11}\text{NO}_5\text{S}$ [$\text{M}+\text{H}$] $^+$ 270.0431 found 270.0431.

4.1.2.17. 3-Oxo-3H-benzof[chromene]-2-sulfonamide (10q).

Prepared from 2-hydroxy-1-naphthaldehyde according to the general procedure; yield: 91 mg (33%). Yellow solid; m. p. >290 °C. ^1H NMR (400 MHz, DMSO- d_6) δ 9.25 (s, 1H), 8.53 (d, J = 8.4 Hz, 1H), 8.34 (d, J = 9.0 Hz, 1H), 8.10 (dd, J = 8.2, 1.3 Hz, 1H), 7.80 (dd, J = 8.4, 7.0, 1.4 Hz, 1H), 7.68 (dd, J = 8.0, 6.9, 1.0 Hz, 1H), 7.64 (d, J = 9.1 Hz, 1H), 7.58 (br.s, 2H). $^{13}\text{C}\{^1\text{H}\}$ NMR (101 MHz, DMSO- d_6) δ 155.8, 155.2, 139.9, 136.5, 130.4, 129.7, 129.6, 129.5, 128.9, 127.1, 122.6, 117.0, 111.9. HRMS (ESI), m/z calcd for $\text{C}_{13}\text{H}_{10}\text{NO}_4\text{S}$ [$\text{M}+\text{H}$] $^+$ 276.0325 found 276.0328.

4.2. Carbonic anhydrase inhibition assay

An Applied Photophysics stopped-flow instrument has been used for assaying the CA catalyzed CO_2 hydration activity [54]. Phenol red (at a concentration of 0.2 mM) has been used as indicator, working at the absorbance maximum of 557 nm, with 20 mM Hepes (pH 7.5) as buffer, and 20 mM Na_2SO_4 (for maintaining constant the ionic

strength), following the initial rates of the CA-catalyzed CO₂ hydration reaction for a period of 10–100 s. The CO₂ concentrations ranged from 1.7 to 17 mM for the determination of the kinetic parameters and inhibition constants. For each inhibitor at least six traces of the initial 5–10% of the reaction have been used for determining the initial velocity. The uncatalyzed rates were determined in the same manner and subtracted from the total observed rates. Stock solutions of inhibitor (0.1 mM) were prepared in distilled–deionized water and dilutions up to 0.01 nM were done thereafter with the assay buffer. Inhibitor and enzyme solutions were preincubated together for 15 min at room temperature prior to assay, in order to allow for the formation of the E–I complex. The inhibition constants were subsequently obtained by nonlinear least-squares methods using PRISM 3 and the Cheng–Prusoff equation, as reported earlier, and represent the mean from at least three different determinations. All CA isoforms were recombinant ones obtained in-house as reported earlier [83–86].

4.3. Cell culture

A431 epidermoid carcinoma, RT4 urinary bladder cancer cell, WI-26 VA4 lung epithelial-like cells were purchased from the ATCC. Primary fibroblasts were purchased from Cell Application Inc. A431 cells and Primary fibroblast cells were maintained in Advanced DMEM (Gibco, UK) supplemented with 5% fetal bovine serum (FBS, Gibco, UK), penicillin (100 UI mL⁻¹), streptomycin (100 µg mL⁻¹) and GlutaMax (3 mM, Gibco, UK). RT4 cells were maintained in McCoy's 5 A media (Gibco, UK) supplemented with 10% fetal bovine serum (FBS, Gibco, UK), penicillin (100 UI mL⁻¹), streptomycin (100 µg mL⁻¹), and GlutaMax (1.5 mM, Gibco, UK). WI-26 VA4 cells were maintained in Advanced MEM (Gibco, UK) supplemented with 5% fetal bovine serum (FBS, Gibco, UK), penicillin (100 UI mL⁻¹), streptomycin (100 µg mL⁻¹), and GlutaMax (1.87 mM, Gibco, UK). All cells line cultivation under a humidified atmosphere of 95% air/5% CO₂ at 37 °C. Subconfluent monolayers, in the log growth phase, were harvested by a brief treatment with TrypLE Express solution (Gibco, UK) in phosphate buffered saline (PBS, Capricorn Scientific, Germany) and washed three times in serum-free PBS. The number of viable cells was determined by trypan blue exclusion.

4.4. Antiproliferative assay (end point)

The effects of the synthesized compounds on cell viability were determined using the MTT colorimetric test. All examined cells were diluted with the growth medium (or medium containing 100 µM CoCl₂ for chemically-induced hypoxia) to 3.5 × 10⁴ cells per mL and the aliquots (7 × 10³ cells per 200 µL) were placed in individual wells in 96-multiplates (Eppendorf, Germany) and incubated for 24 h. The next day the cells were then treated with synthesized compounds separately concentration 100 µM and incubated for 24 h at 37 °C in 5% CO₂ atmosphere. Each compound was tested in triplicate. After incubation, the cells were then treated with 40 µL MTT solution (3-(4,5-dimethylthiazol-2-yl)-2,5-diphenyltetrazolium bromide, 5 mg mL⁻¹ in PBS) and incubated 4 h. After an additional 4 h incubation, the medium with MTT was removed and DMSO (150 µL) was added to dissolve the crystals formazan. The plates were shaken for 10 min. The optical density of each well was determined at 560 nm using a microplate reader GloMax Multi+ (Promega, USA). Each of the tested compounds was evaluated for cytotoxicity in three separate experiments.

4.5. MTT assay

All examined cells were diluted with the growth medium (or medium containing 100 µM CoCl₂ for chemically-induced hypoxia)

to 3.5 × 10⁴ cells per mL and the aliquots (7 × 10³ cells per 200 µL) were placed in individual wells in 96-multiplates (Eppendorf, Germany) and incubated for 24 h. Triplicate wells were treated with test compounds starting at 200.0 µM concentration and diluted at various concentrations or DMSO (Sigma, USA) as control with final concentration 0.1%. Plates were incubated for 72 h (or 24 h, 48 h) at 37 °C in 5% CO₂ atmosphere. After incubation, the cells were then treated with 40 µL MTT solution (3-(4,5-dimethylthiazol-2-yl)-2,5-diphenyltetrazolium bromide, 5 mg mL⁻¹ in PBS) and incubated 4 h. After an additional 4 h incubation, the medium with MTT was removed and DMSO (150 µL) was added to dissolve the crystals formazan. The plates were shaken for 10 min. The optical density of each well was determined at 560 nm using a microplate reader GloMax Multi+ (Promega, USA). Each of the tested compounds was evaluated for cytotoxicity in three separate experiments.

4.6. Apoptosis assay

For the detection of apoptosis, the cells were plated at 6-well culture plates (Eppendorf, Germany) and allowed to grow overnight. After the cells reached subconfluency, the medium was replaced with tested compounds (5 ... 25 µM). The exposed cells were placed at 37 °C in a 5% CO₂ incubator for 24 h. The cultured cells were washed twice with PBS and resuspended in 1 × binding buffer (AnnexinV-FITC kit, Invitrogen, USA) at a concentration 1 × 10⁶ mL⁻¹. Annexin FITC (5 µL) and propidium iodide (PI, 2 µL) were added to 100 µL of the cell suspension and incubated for 15 min at room temperature (25 °C) in the dark. After incubation 400 µL of 1 × binding buffer was added to each tube and the stained cells were analyzed within 1 h using CytoFlex (Beckham Culture, USA) and CytExpert 2.1 program. Since, Annexin V FITC staining precedes the loss of membrane integrity that accompanies the later stage identified by PI, Annexin FITC positive, PI negative indicates early apoptosis, while the viable cells are Annexin V FITC negative, PI negative. The cells that are in late apoptosis, or dead are both Annexin V FITC and PI positive.

4.7. Caspase 3/7 assay

For the detection of caspase 3/7 activation, the cells were plated at 6-well culture plates (Eppendorf, Germany) and allowed to grow overnight. After the cells reached subconfluency, the medium was replaced with tested compounds (5 ... 25 µM). The exposed cells were placed at 37 °C in a 5% CO₂ incubator for 24 h. The cultured cells were washed twice with PBS and resuspended in 1 mL fresh PBS at a concentration 1 × 10⁶ mL⁻¹. Diluted the CellEvent™ Caspase-3/7 Green Detection Reagent into cells suspension to a final concentration of 4 µM and incubated for 30 min at 37 °C in a 5% CO₂ incubator. After incubation, stained cells were analyzed within 20 min using CytoFlex (Beckham Culture, USA) and CytExpert 2.1 program.

Declaration of competing interest

The authors declare that they have no known competing financial interests or personal relationships that could have appeared to influence the work reported in this paper.

Acknowledgements

This research was supported by the Russian Science Foundation (project grant 21-73-20264). We are grateful to the Centre for Chemical Analysis and Materials Research of Saint Petersburg State University Research Park for the high-resolution mass-spectrometry data.

Appendix A. Supplementary data

Supplementary data to this article can be found online at <https://doi.org/10.1016/j.ejmech.2021.113589>.

References

- J.R. Casey, Why bicarbonate? *Biochem. Cell Biol. Biochem Cell Biol*, 2006, pp. 930–939, <https://doi.org/10.1139/O06-184>.
- C.T. Supuran, Structure and function of carbonic anhydrases, *Biochem. J.* 473 (2016) 2023–2032, <https://doi.org/10.1042/BCJ20160115>.
- C.D. Boone, M. Pinard, R. McKenna, D. Silverman, Catalytic mechanism of α -class carbonic anhydrases: CO₂ hydration and proton transfer, *Subcell. Biochem.* 75 (2014) 31–52, https://doi.org/10.1007/978-94-007-7359-2_3.
- C.T. Supuran, C. Capasso, An overview of the bacterial carbonic anhydrases, *Metabolites* 7 (2017) 56, <https://doi.org/10.3390/metabo7040056>.
- A. Angeli, M. Pinteala, S.S. Maier, S. Del Prete, C. Capasso, B.C. Simionescu, C.T. Supuran, Inhibition of α -, β -, γ -, δ -, ζ - and η -class carbonic anhydrases from bacteria, fungi, algae, diatoms and protozoans with famotidine, *J. Enzym. Inhib. Med. Chem.* 34 (2019) 644–650, <https://doi.org/10.1080/14756366.2019.1571273>.
- E. Berrino, M. Bozdog, S. Del Prete, F.A.S. Alasmari, L.S. Alqahtani, Z. Althman, C. Capasso, C.T. Supuran, Inhibition of α -, β -, γ -, and δ -carbonic anhydrases from bacteria and diatoms with *N*'-aryl-*N*'-hydroxy-ureas, *J. Enzym. Inhib. Med. Chem.* 33 (2018) 1194–1198, <https://doi.org/10.1080/14756366.2018.1490733>.
- V. De Luca, A. Petreni, A. Nocentini, A. Scaloni, C.T. Supuran, C. Capasso, Effect of sulfonamides and their structurally related derivatives on the activity of α -carbonic anhydrase from *Burkholderia territorii*, *Int. J. Mol. Sci.* 22 (2021) 1–13, <https://doi.org/10.3390/ijms22020571>.
- S. Del Prete, V. De Luca, G. De Simone, C.T. Supuran, C. Capasso, Cloning, expression and purification of the complete domain of the η -carbonic anhydrase from *Plasmodium falciparum*, *J. Enzym. Inhib. Med. Chem.* 31 (2016) 54–59, <https://doi.org/10.1080/14756366.2016.1217856>.
- R. McKenna, C.T. Supuran, Carbonic anhydrase inhibitors drug design, *Subcell. Biochem.* 75 (2014) 291–323, https://doi.org/10.1007/978-94-007-7359-2_15.
- C.T. Supuran, Structure-based drug discovery of carbonic anhydrase inhibitors, *J. Enzym. Inhib. Med. Chem.* 27 (2012) 759–772, <https://doi.org/10.3109/14756366.2012.672983>.
- K.M. Gilmour, Perspectives on carbonic anhydrase, *Comp. Biochem. Physiol. Mol. Integr. Physiol.* 157 (2010) 193–197, <https://doi.org/10.1016/j.cbpa.2010.06.161>.
- M.E. McDevitt, L.A. Lambert, Molecular evolution and selection pressure in alpha-class carbonic anhydrase family members, *Biochim. Biophys. Acta Protein Proteomics* 1814 (2011) 1854–1861, <https://doi.org/10.1016/j.bbapap.2011.07.007>.
- S. Pastorekova, R.J. Gillies, The role of carbonic anhydrase IX in cancer development: links to hypoxia, acidosis, and beyond, *Canc. Metastasis Rev.* 38 (2019) 65–77, <https://doi.org/10.1007/s10555-019-09799-0>.
- S. Zamanova, A.M. Shabana, U.K. Mondal, M.A. Ilies, Carbonic anhydrases as disease markers, *Expert Opin. Ther. Pat.* 29 (2019) 509–533, <https://doi.org/10.1080/13543776.2019.1629419>.
- C. Supuran, Carbonic anhydrases as drug targets - an overview, *Curr. Top. Med. Chem.* 7 (2007) 825–833, <https://doi.org/10.2174/156802607780636690>.
- S. Kalinin, A. Valtari, M. Ruponen, E. Toropainen, A. Kovalenko, A. Nocentini, M. Gureev, D. Dar'in, A. Urtti, C.T. Supuran, M. Krasavin, Highly hydrophilic 1,3-oxazol-5-yl benzenesulfonamide inhibitors of carbonic anhydrase II for reduction of glaucoma-related intraocular pressure, *Bioorg. Med. Chem.* 27 (2019), <https://doi.org/10.1016/j.bmc.2019.115086>.
- A. Nocentini, C.T. Supuran, Carbonic anhydrase inhibitors for the treatment of neuropathic pain and arthritis, *Carbon. Anhydrases Biochem. Pharmacol. An Evergr. Pharm. Target*, Elsevier, 2019, pp. 367–386, <https://doi.org/10.1016/B978-0-12-816476-1.00017-4>.
- C.T. Supuran, Carbonic anhydrase inhibitors as emerging drugs for the treatment of obesity, *Expet Opin. Emerg. Drugs* 17 (2012) 11–15, <https://doi.org/10.1517/14728214.2012.664132>.
- A. Scozzafava, C.T. Supuran, Glaucoma and the applications of carbonic anhydrase inhibitors, *Subcell. Biochem.* 75 (2014) 349–359, https://doi.org/10.1007/978-94-007-7359-2_17.
- C.T. Supuran, Carbonic anhydrases: novel therapeutic applications for inhibitors and activators, *Nat. Rev. Drug Discov.* 7 (2008) 168–181, <https://doi.org/10.1038/nrd2467>.
- C.T. Supuran, α -Experimental carbonic anhydrase inhibitors for the treatment of hypoxic tumors α -, *J. Exp. Pharmacol.* 12 (2020) 603–617, <https://doi.org/10.2147/JEP.S265620>.
- I.S. Ismail, The role of carbonic anhydrase in hepatic glucose production, *Curr. Diabetes Rev.* 14 (2018) 108–112, <https://doi.org/10.2174/1573399812666161214122351>.
- P. Blandina, G. Provensi, M.B. Passani, C. Capasso, C.T. Supuran, Carbonic anhydrase modulation of emotional memory. Implications for the treatment of cognitive disorders, *J. Enzym. Inhib. Med. Chem.* 35 (2020) 1206–1214, <https://doi.org/10.1080/14756366.2020.1766455>.
- A. Angeli, F. Carta, A. Nocentini, J.-Y. Winum, R. Zalubovskis, A. Akdemir, V. Onnis, W.M. Eldehna, C. Capasso, G. De Simone, S.M. Monti, S. Carradori, W.A. Donald, S. Dedhar, C.T. Supuran, Carbonic anhydrase inhibitors targeting metabolism and tumor microenvironment, *Metabolites* 10 (2020) 412, <https://doi.org/10.3390/metabo10100412>.
- H.M. Becker, J.W. Deitmer, Proton transport in cancer cells: the role of carbonic anhydrases, *Int. J. Mol. Sci.* 22 (2021) 1–17, <https://doi.org/10.3390/ijms22063171>.
- K.F. Tonissen, S.-A. Poulsen, Carbonic anhydrase XII inhibition overcomes P-glycoprotein-mediated drug resistance: a potential new combination therapy in cancer, *Cancer Drug Resist* 4 (2021), <https://doi.org/10.20517/cdr.2020.110>.
- M.Y. Mboge, B.P. Mahon, R. McKenna, S.C. Frost, Carbonic anhydrases: role in pH control and cancer, *Metabolites* 8 (2018), <https://doi.org/10.3390/metabo8010019>.
- M.Y. Mboge, R. McKenna, S.C. Frost, Advances in anti-cancer drug development targeting carbonic anhydrase IX and XII. *Top. Anti-cancer Res.*, BENTHAM SCIENCE PUBLISHERS, 2016, pp. 3–42, <https://doi.org/10.2174/9781681083339116050004>.
- C.T. Supuran, Carbonic anhydrase inhibitors as emerging agents for the treatment and imaging of hypoxic tumors, *Expet Opin. Invest. Drugs* 27 (2018) 963–970, <https://doi.org/10.1080/13543784.2018.1548608>.
- J. Lau, K. Lin, F. Bénard, Past, present, and future: development of theranostic agents targeting carbonic anhydrase IX, *Theranostics* 7 (2017), <https://doi.org/10.7150/thno.21848>.
- V. Burianova, S. Kalinin, C.T. Supuran, M. Krasavin, Radiotracers for positron emission tomography (PET) targeting tumour-associated carbonic anhydrase isoforms, *Eur. J. Med. Chem.* (2020), <https://doi.org/10.1016/j.ejmech.2020.113046>.
- M.A. Pinard, B. Mahon, R. McKenna, Probing the surface of human carbonic anhydrase for clues towards the design of isoform specific inhibitors, *BioMed Res. Int.* 2015 (2015) 453543, <https://doi.org/10.1155/2015/453543>.
- C.T. Supuran, How many carbonic anhydrase inhibition mechanisms exist? *J. Enzym. Inhib. Med. Chem.* 31 (2016) 345–360, <https://doi.org/10.3109/14756366.2015.1122001>.
- M. Bozdog, M. Ferraroni, E. Nuti, D. Vullo, A. Rossello, F. Carta, A. Scozzafava, C.T. Supuran, Combining the tail and the ring approaches for obtaining potent and isoform-selective carbonic anhydrase inhibitors: solution and X-ray crystallographic studies, *Bioorg. Med. Chem.* 22 (2014) 334–340, <https://doi.org/10.1016/j.bmc.2013.11.016>.
- A. Bonardi, A. Nocentini, S. Bua, J. Combs, C. Lomelino, J. Andring, L. Lucarini, S. Sgambellone, E. Masini, R. McKenna, P. Gratteri, C.T. Supuran, Sulfonamide inhibitors of human carbonic anhydrases designed through a three-tails approach: improving ligand/isoform matching and selectivity of action, *J. Med. Chem.* 63 (2020) 7422–7444, <https://doi.org/10.1021/acs.jmedchem.0c00733>.
- A. Bhatt, B.P. Mahon, V.W.D. Cruzeiro, B. Cornelio, M. Laronze-Cochard, M. Ceruso, J. Sapi, G.A. Rance, A.N. Kholobystov, A. Fontana, A. Roitberg, C.T. Supuran, R. McKenna, Structure–activity relationships of benzenesulfonamide-based inhibitors towards carbonic anhydrase isoform specificity, *Chembiochem* 18 (2017) 213–222, <https://doi.org/10.1002/cbic.201600513>.
- A. Maresca, C. Temperini, L. Pochet, B. Masereel, A. Scozzafava, C.T. Supuran, Deciphering the mechanism of carbonic anhydrase inhibition with coumarins and thiocoumarins, *J. Med. Chem.* 53 (2010) 335–344, <https://doi.org/10.1021/jm901287j>.
- G. De Simone, V. Alterio, C.T. Supuran, Exploiting the hydrophobic and hydrophilic binding sites for designing carbonic anhydrase inhibitors, *Expet Opin. Drug Discov.* 8 (2013) 793–810, <https://doi.org/10.1517/17460441.2013.795145>.
- R. Meleddu, S. Deplano, E. Maccioni, F. Ortuso, F. Cottiglia, D. Secci, A. Onali, E. Sanna, A. Angeli, R. Angius, S. Alcaro, C.T. Supuran, S. Distinto, Selective inhibition of carbonic anhydrase IX and XII by coumarin and psoralen derivatives, *J. Enzym. Inhib. Med. Chem.* 36 (2021) 685–692, <https://doi.org/10.1080/14756366.2021.1887171>.
- M. Krasavin, R. Zalubovskis, A. Grandane, I. Domračeva, P. Zhmurov, C.T. Supuran, Sulfocoumarins as dual inhibitors of human carbonic anhydrase isoforms IX/XII and of human thioredoxin reductase, *J. Enzym. Inhib. Med. Chem.* 35 (2020) 506–510, <https://doi.org/10.1080/14756366.2020.1712596>.
- N. Touisni, A. Maresca, P.C. McDonald, Y. Lou, A. Scozzafava, S. Dedhar, J.Y. Winum, C.T. Supuran, Glycosyl coumarin carbonic anhydrase IX and XII inhibitors strongly attenuate the growth of primary breast tumors, *J. Med. Chem.* 54 (2011) 8271–8277, <https://doi.org/10.1021/jm200983e>.
- A. Thiry, M. Ledecq, A. Cecchi, J.M. Dogné, J. Wouters, C.T. Supuran, B. Masereel, Indanesulfonamides as carbonic anhydrase inhibitors. Toward structure-based design of selective inhibitors of the tumor-associated isozyme CA IX, *J. Med. Chem.* 49 (2006) 2743–2749, <https://doi.org/10.1021/jm0600287>.
- N. Chandak, M. Ceruso, C.T. Supuran, P.K. Sharma, Novel sulfonamide bearing coumarin scaffolds as selective inhibitors of tumor associated carbonic anhydrase isoforms IX and XII, *Bioorg. Med. Chem.* 24 (2016) 2882–2886, <https://doi.org/10.1016/j.bmc.2016.04.052>.
- J. Wagner, B.S. Avvaru, A.H. Robbins, A. Scozzafava, C.T. Supuran, R. McKenna, Coumarinyl-substituted sulfonamides strongly inhibit several human carbonic anhydrase isoforms: solution and crystallographic investigations,

- Bioorg. Med. Chem. 18 (2010) 4873–4878, <https://doi.org/10.1016/j.bmc.2010.06.028>.
- [45] M.A. Abdelrahman, H.S. Ibrahim, A. Nocentini, W.M. Eldehna, A. Bonardi, H.A. Abdel-Aziz, P. Gratteri, S.M. Abou-Seri, C.T. Supuran, Novel 3-substituted coumarins as selective human carbonic anhydrase IX and XII inhibitors: synthesis, biological and molecular dynamics analysis, *Eur. J. Med. Chem.* 209 (2021) 112897, <https://doi.org/10.1016/j.ejmech.2020.112897>.
- [46] Z.C. Wang, Y.J. Qin, P.F. Wang, Y.A. Yang, Q. Wen, X. Zhang, H.Y. Qiu, Y.T. Duan, Y.T. Wang, Y.L. Sang, H.L. Zhu, Sulfonamides containing coumarin moieties selectively and potentially inhibit carbonic anhydrases II and IX: design, synthesis, inhibitory activity and 3D-QSAR analysis, *Eur. J. Med. Chem.* 66 (2013) 1–11, <https://doi.org/10.1016/j.ejmech.2013.04.035>.
- [47] B.Z. Kurt, F. Sönmez, Ç. Bilen, A. Ergun, N. Gençer, O. Arslan, M. Kucukislamoglu, Synthesis, antioxidant and carbonic anhydrase I and II inhibitory activities of novel sulphonamide-substituted coumarylthiazole derivatives, *J. Enzym. Inhib. Med. Chem.* 31 (2016) 991–998, <https://doi.org/10.3109/14756366.2015.1077823>.
- [48] A. Irfan, L. Rubab, M.U. Rehman, R. Anjum, S. Ullah, M. Marjana, S. Qadeer, S. Sana, Coumarin sulfonamide derivatives: an emerging class of therapeutic agents, *Heterocycl. Commun.* 26 (2020) 46–59, <https://doi.org/10.1515/hc-2020-0008>.
- [49] M. Walles, A. Connor, D. Hainzl, ADME and safety aspects of non-cleavable linkers in drug discovery and development, *Curr. Top. Med. Chem.* 17 (2018) 3463–3475, <https://doi.org/10.2174/156802661866618118153502>.
- [50] J.M. Contreras, J.J. Bourguignon, Identical and non-identical twin drugs. *Pract. Med. Chem.*, second ed., Elsevier Inc., 2003, pp. 251–273, <https://doi.org/10.1016/B978-012744481-9/50020-9>.
- [51] 692 E. Knoevenagel, R. Arnot, Condensation von Salicylaldehyd mit Cyanessigester, Benzoylessigester und Acetylaceton, *Berichte Der Dtsch. Chem. Gesellschaft.* 37 (1904) 4496–4502, <https://doi.org/10.1002/ber.19040370442>.
- [52] B.C. Ranu, R. Jana, Ionic liquid as catalyst and reaction medium – a simple, efficient and green procedure for Knoevenagel condensation of aliphatic and aromatic carbonyl compounds using a task-specific basic ionic liquid, *Eur. J. Org. Chem.* (2006) 3767–3770, <https://doi.org/10.1002/ejoc.200600335>, 2006.
- [53] S.F. Britcher, D.W. Cochran, B.T. Phillips, J.P. Springer, W.C. Lumma, Direct synthesis of trisubstituted isothiazole 1,1-dioxides. Regioselective substitution reactions at C-3 and C-4, *J. Org. Chem.* 48 (1983) 763–767, <https://doi.org/10.1021/jo00154a001>.
- [54] R.G. Khalifah, The carbon dioxide hydration activity of carbonic anhydrase, *J. Biol. Chem.* 246 (1971) 2561–2573, <http://www.jbc.org/content/246/8/2561>.
- [55] S. Pastorekova, S. Parkkila, J. Pastorek, C.T. Supuran, Carbonic anhydrases: current state of the art, therapeutic applications and future prospects, *J. Enzym. Inhib. Med. Chem.* 19 (2004) 199–229, <https://doi.org/10.1080/14756360410001689540>.
- [56] S. Dong Soo, P. Won Young, K. Ki Hyung, K. Ahrong, K. Young Keum, K. Kyungbin, C. Kyung Un, Differential regulation and prognostic significance of endogenous hypoxic markers in endometrial carcinomas, *Eur. J. Gynaecol. Oncol.* 39 (2018) 773–778.
- [57] C.T. Supuran, Therapeutic applications of the carbonic anhydrase inhibitors, *Therapy* 4 (2007) 355–378, <https://doi.org/10.2217/14750708.4.3.355>.
- [58] M.A. Pinar, B. Mahon, R. McKenna, Probing the surface of human carbonic anhydrase for clues towards the design of isoform specific inhibitors, *BioMed Res. Int.* 2015 (2015), <https://doi.org/10.1155/2015/453543>.
- [59] C.T. Supuran, V. Alterio, A. Di Fiore, K. D' Ambrosio, F. Carta, S.M. Monti, G. De Simone, Inhibition of carbonic anhydrase IX targets primary tumors, metastases, and cancer stem cells: three for the price of one, *Med. Res. Rev.* 38 (2018) 1799–1836, <https://doi.org/10.1002/med.21497>.
- [60] R. Baghban, L. Roshangar, R. Jahanban-Esfahlan, K. Seidi, A. Ebrahimi-Kalan, M. Jaymand, S. Kolahian, T. Javaheri, P. Zare, Tumor microenvironment complexity and therapeutic implications at a glance, *Cell Commun. Signal.* 18 (2020), <https://doi.org/10.1186/s12964-020-0530-4>.
- [61] P. Ebbesen, E.O. Pettersen, T.A. Gorr, G. Jobst, K. Williams, J. Kieninger, R.H. Wenger, S. Pastorekova, L. Dubois, P. Lambin, B.G. Wouters, T. Van Den Beucken, C.T. Supuran, L. Poellinger, P. Ratcliffe, A. Kanopka, A. Görlach, M. Gasmann, A.L. Harris, P. Maxwell, A. Scozzafava, Taking advantage of tumor cell adaptations to hypoxia for developing new tumor markers and treatment strategies, *J. Enzym. Inhib. Med. Chem.* 24 (2009) 1–39, <https://doi.org/10.1080/14756360902784425>.
- [62] A. Waheed, W.S. Sly, Carbonic anhydrase XII functions in health and disease, *Gene* 623 (2017) 33–40, <https://doi.org/10.1016/j.gene.2017.04.027>.
- [63] G. Ilardi, N. Zambrano, F. Merolla, M. Siano, S. Varricchio, M. Vecchione, G. Rosa, M. Mascolo, S. Staibano, Histopathological determinants of tumor resistance: a special look to the immunohistochemical expression of carbonic anhydrase IX in human cancers, *Curr. Med. Chem.* 21 (2014) 1569–1582, <https://doi.org/10.2174/09298673113209990227>.
- [64] Inhibition of Carbonic anhydrase in combination with platinum and etoposide-based radiochemotherapy in patients with localized small cell lung cancer - full text view - ClinicalTrials.gov, accessed April 20, 2021, <https://clinicaltrials.gov/ct2/show/NCT03467360>.
- [65] Trial to determine optimal phase II dose of the oral dual CAIX inhibitor/radiosensitizer - full text view - ClinicalTrials.gov, accessed April 20, 2021, <https://clinicaltrials.gov/ct2/show/NCT02216669?term=carbonic+anhydrase&draw=4>.
- [66] A study of SLC-0111 and gemcitabine for metastatic pancreatic ductal cancer in subjects positive for CAIX - full text view - ClinicalTrials.gov, accessed April 20, 2021, <https://www.clinicaltrials.gov/ct2/show/NCT03450018?term=SLC-0111>.
- [67] M. Krasavin, S. Kalinin, T. Sharonova, C.T. Supuran, Inhibitory activity against carbonic anhydrase IX and XII as a candidate selection criterion in the development of new anticancer agents, *J. Enzym. Inhib. Med. Chem.* 35 (2020) 1555–1561, <https://doi.org/10.1080/14756366.2020.1801674>.
- [68] S. Pastorekova, R.J. Gillies, The role of carbonic anhydrase IX in cancer development: links to hypoxia, acidosis, and beyond, *Canc. Metastasis Rev.* 38 (2019) 65–77, <https://doi.org/10.1007/s10555-019-09799-0>.
- [69] C.Y. Chu, Y.T. Jin, W. Zhang, J. Yu, H.P. Yang, H.Y. Wang, Z.J. Zhang, X.P. Liu, Q. Zou, CA IX is upregulated in CoCl₂-induced hypoxia and associated with cell invasive potential and a poor prognosis of breast cancer, *Int. J. Oncol.* 48 (2016) 271–280, <https://doi.org/10.3892/ijo.2015.3253>.
- [70] A. Rescifina, M.G. Varrica, C. Carnovale, G. Romeo, U. Chiacchio, Novel isoxazole polycyclic aromatic hydrocarbons as DNA-intercalating agents, *Eur. J. Med. Chem.* 51 (2012) 163–173, <https://doi.org/10.1016/j.ejmech.2012.02.038>.
- [71] D. Bandyopadhyay, J.C. Granados, J.D. Short, B.K. Banik, Polycyclic aromatic compounds as anticancer agents: evaluation of synthesis and in vitro cytotoxicity, *Oncol. Lett.* 3 (2012) 45–49, <https://doi.org/10.3892/ol.2011.436>.
- [72] F.F. Becker, B.K. Banik, Polycyclic aromatic compounds as anticancer agents: synthesis and biological evaluation of methoxy dibenzofluorene derivatives, *Front. Chem.* 2 (2014) 55, <https://doi.org/10.3389/fchem.2014.00055>.
- [73] V. Sharma, M. Gupta, P. Kumar, A. Sharma, A comprehensive review on fused heterocyclic as DNA intercalators: promising anticancer agents, *Curr. Pharmaceut. Des.* 27 (2021) 15–42, <https://doi.org/10.2174/138161282666201118113311>.
- [74] K.H. Khan, M. Blanco-Codesido, L.R. Mofife, Cancer therapeutics: targeting the apoptotic pathway, *Crit. Rev. Oncol. Hematol.* 90 (2014) 200–219, <https://doi.org/10.1016/j.critrevonc.2013.12.012>.
- [75] J.A. Call, S.G. Eckhardt, D.R. Camidge, Targeted manipulation of apoptosis in cancer treatment, *Lancet Oncol.* 9 (2008) 1002–1011, [https://doi.org/10.1016/S1470-2045\(08\)70209-2](https://doi.org/10.1016/S1470-2045(08)70209-2).
- [76] F. Cianchi, M.C. Vinci, C.T. Supuran, B. Peruzzi, P. De Giuli, G. Fasolis, G. Perigli, S. Pastorekova, L. Papucci, A. Pini, E. Masini, L. Puccetti, Selective inhibition of carbonic anhydrase IX decreases cell proliferation and induces ceramide-mediated apoptosis in human cancer cells, *J. Pharmacol. Exp. Therapeut.* 334 (2010) 710–719, <https://doi.org/10.1124/jpet.110.167270>.
- [77] I. Koyuncu, A. Gönül, A. Kocyigit, E. Temiz, M. Durgun, C.T. Supuran, Selective inhibition of carbonic anhydrase-IX by sulphonamide derivatives induces pH and reactive oxygen species-mediated apoptosis in cervical cancer HeLa cells, *J. Enzym. Inhib. Med. Chem.* 33 (2018) 1137–1149, <https://doi.org/10.1080/14756366.2018.1481403>.
- [78] A. Sabt, O.M. Abdelhafez, R.S. El-Haggag, H.M.F. Madkour, W.M. Eldehna, E.E.D.A.M. El-Khrisy, M.A. Abdel-Rahman, L.A. Rashed, Novel coumarin-6-sulfonamides as apoptotic anti-proliferative agents: synthesis, in vitro biological evaluation, and QSAR studies, *J. Enzym. Inhib. Med. Chem.* 33 (2018) 1095–1107, <https://doi.org/10.1080/14756366.2018.1477137>.
- [79] J. Zhang, Y. Tan, G. Li, L. Chen, M. Nie, Z. Wang, H. Ji, Coumarin sulfonamides and amides derivatives: design, synthesis, and antitumor activity in vitro, *Molecules* 26 (2021), <https://doi.org/10.3390/molecules26040786>.
- [80] B.A. Carneiro, W.S. El-Deiry, Targeting apoptosis in cancer therapy, *Nat. Rev. Clin. Oncol.* 17 (2020) 395–417, <https://doi.org/10.1038/s41571-020-0341-y>.
- [81] S.A. Wolckenhauer, A.S. Devlin, J. Du Bois, δ-Sultone formation through Rh-catalyzed C-H insertion, *Org. Lett.* 9 (2007) 4363–4366, <https://doi.org/10.1021/ol701950d>.
- [82] L. Cao, K. Weidner, P. Renaud, Metal-free, radical addition to alkenes via desulfurative chlorine atom transfer, *Adv. Synth. Catal.* 353 (2011) 3467–3472, <https://doi.org/10.1002/adsc.201100473>.
- [83] B.L. Wilkinson, L.F. Bornaghi, T.A. Houston, A. Innocente, C.T. Supuran, S.A. Poulsen, A novel class of carbonic anhydrase inhibitors: glycoconjugate benzene sulfonamides prepared by “click-tailing”, *J. Med. Chem.* 49 (2006) 6539–6548, <https://doi.org/10.1021/jm060967z>.
- [84] M. Lopez, A.J. Salmon, C.T. Supuran, S.-A. Poulsen, Carbonic anhydrase inhibitors developed through “click tailing”, *Curr. Pharmaceut. Des.* 16 (2010) 3277–3287, <https://doi.org/10.2174/138161210793429869>.
- [85] B.L. Wilkinson, L.F. Bornaghi, T.A. Houston, A. Innocenti, D. Vullo, C.T. Supuran, S.A. Poulsen, Carbonic anhydrase inhibitors: inhibition of isozymes I, II, and IX with triazole-linked O-glycosides of benzene sulfonamides, *J. Med. Chem.* 50 (2007) 1651–1657, <https://doi.org/10.1021/jm061320h>.
- [86] N. Pala, L. Micheletto, M. Sechi, M. Aggarwal, F. Carta, R. McKenna, C.T. Supuran, Carbonic anhydrase inhibition with benzenesulfonamides and tetrafluorobenzenesulfonamides obtained via click chemistry, *ACS Med. Chem. Lett.* 5 (2014) 927–930, <https://doi.org/10.1021/ml500196t>.